70-21,823

BURGETT, Charley Ballard, 1940-
LUMINESCENCE AND PHOTOCONDUCTIVITY IN COPPER
DOPED ZINC SULFIDE AND CADMIUM SULFIDE.

The University of Oklahoma, Ph.D., 1970
Physics, general

University Microfilms, A XEROX Company, Ann Arbor, Michigan

THE UNIVERSITY OF OKLAHOMA

GRADUATE COLLEGE

# LUMINESCENCE AND PHOTOCONDUCTIVITY IN COPPER DOPED ZINC SULFIDE AND CADMIUM SULFIDE

A DISSERTATION
SUBMITTED TO THE GRADUATE FACULTY
in partial fulfillment of the requirements for the
degree of
DOCTOR OF PHILOSOPHY

BY
CHARLEY BALLARD BURGETT
1970

# LUMINESCENCE AND PHOTOCONDUCTIVITY IN COPPER DOPED ZINC SULFIDE AND CADMIUM SULFIDE

APPROVED BY

Chun C. Lin

Stanley E. Babb, Jr.

Charles J. Mankin

Robert M. St. John

DISSERTATION COMMITTEE

# ACKNOWLEDGEMENTS

The author wishes to express his sincere appreciation to Professor Chun Chia Lin, upon whose suggestions and guidance this work is based.

Financial support for the 1963 through 1966 academic years was generously provided by the National Aeronautics and Space Administration under the Graduate Traineeship program.

A very profound expression of gratitude is extended to my wife, Karen, for her cheerfulness, patience, and help in the preparation of this manuscript.

# TABLE OF CONTENTS

## TABLE OF CONTENTS (continued)

Page

Chapter

IV. (continued)

## LIST OF ILLUSTRATIONS

## LIST OF ILLUSTRATIONS (continued)

## LIST OF ILLUSTRATIONS (continued)

# LUMINESCENCE AND PHOTOCONDUCTIVITY IN COPPER DOPED ZINC SULFIDE AND CADMIUM SULFIDE

## CHAPTER I

### I. Introduction

The luminescence of ZnS crystals has been a subject of interest for over fifty years. Although various models have been proposed to explain the mechanism of the luminescence, only in recent years have serious attempts been made to describe the electronic processes in terms of the atomic constituents of the crystals.

The green luminescence has been thought of as transitions to the $Cu^{++}$ impurity centers from electrons in the conduction band or electrons trapped in shallow donor levels (1,2). Shionoya and his co-workers (3,4,5) have recently proposed the unassociated donor-acceptor pair emission mechanism for the green luminescence, i.e., transition from a coactivator donor level to the Cu acceptor level. According to the crystal field theory, the ground state $3d^9$ of a free $Cu^{++}$ ion is split into two levels in a tetrahedral crystal lattice and the spacing between these two levels was found to be about 5,800 $cm^{-1}$ in the case of ZnO (6). Indeed, the recent work of Broser, Maier, and Schulz (7), has established that the infrared (i.r.) luminescence near 1.5μ and the absorption at 1.3μ are due to the transitions between these two crystal field levels. Although the hole in $Cu^{++}$ is normally located in the upper level which is responsible for the green luminescence, the presence of the lower level or the $Cu^{++}$ center suggests the possibility of optical quenching effects other than the 0.8μ band (1,8,9) and the strong correlation between the green and the i.r. luminescence.

In this thesis we shall report some studies of quenching of the green luminescence of the ZnS and its counterpart in CdS crystals with special reference to the energy levels of the Cu center. Infrared quenching of the photo-Hall effect has also been examined in conjunction with the luminescence experiment. The results of this work have shown that the stimulation of the green and infrared luminescence can be explained by Shionoya's unassociated pair model and that the three different infrared quenching modes of the green luminescence can all be attributed to the crystal field energy levels of the Cu center, and that the strong resemblance of the quenching of the green luminescence and the excitation of the infrared emission can be explained by a combination of the unassociated pair model and the energy level of the Cu center.

## II. Properties of ZnS and CdS

Anticipating the discussions on luminescence and photoconductivity, there are several topics which are common to both and will be covered as a preface to the main discussion.

The characterization of the pure compounds, and of impurities incorporated in the pure compounds is principal to both photoconductivity and luminescence. Also optical excitation of carriers by various mechanisms will be covered, and a comparison of optical and electron beam excitation.

## Pure ZnS and CdS

The properties of pure ZnS and CdS which will be of interest in the discussions of photoconductivity are the band gap, free carrier mobilities and lifetimes, and common native defects. Properties associated with incorporation of impurities will also be important: energy levels and valency of different impurity types, and their effect on luminescence and photoconductivity.

The II-VI compounds are intermediate between elemental semiconductors which are purely covalent, and those compounds which have purely ionic bonding. Estimates of about 50 per cent to 90 per cent ionic bonding in ZnS (10) have been made. Cadmium sulfide is probably even more ionic, about 85 per cent to 90 per cent.

The band gaps of ZnS and CdS are 3.7 and 2.4 eV respectively, at room temperature; the band structure near $k = 0$ is shown in Figure 1-1. The valence band is triply degenerate, but split by spin orbit coupling.

A continuous series of intermediate Zn and Cd sulfides can be formed, denoted by $Zn_x\ Cd_{x-1}\ S$. The band gap, photoconductivity peaks and luminescence peaks shift continuously to lower energies with increasing Cd concentration.

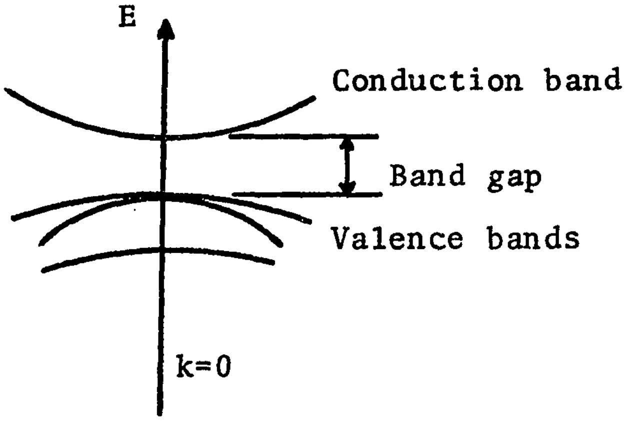

Figure 1-1. Band structure for Wurtzite near k = 0.

## Free Carrier Lifetime and Mobility

Electron mobilities in ZnS and CdS fall in the range of 100 to 200 $cm^2$/volt-sec. in pure samples. Values for hole mobilities are lower and not well documented. Electron and hole lifetimes in pure samples are in the range of one microsecond; carrier lifetime will be seen to change by many orders of magnitude with incorporation of certain impurities, having a pronounced effect on photoconductivity.

## Impurities

It is known that group III and group VII elements create shallow donor centers in II-VI compounds. For example, Cl can enter substitutionally on anion (sulfur) sites, and since it has seven valence electrons compared to sulfur's six, acts as a donor, i.e., it easily gives up one electron to the conduction band. The energy level produced by halogens is about 0.25 eV below the conduction band in zinc sulfide and about

0.03 eV in cadmium sulfide (11).

Group III elements, Al, Ga, In, Sc, enter substitutionally on cation sites, acting as donors, with an energy level about 0.5 eV below the conduction band.

Group IB elements Cu, Ag, Au, having one valence electron (e.g., Cu, $(3d)^{10}(4s)$), substituting for divalent cations, act as acceptors. In the ionic picture Zn or Cd supply the two valence electrons to anions. Hence, for monovalent ions $Cu^+$, etc., on Zn or Cd sites will supply only one electron, leaving a "hole" at that lattice site.

However, Cu, Ag, and Au easily form doubly ionized ions $Cu^{++}$, etc., and supply the necessary two bonding electrons, producing $Cu^{++}(3d)^9$. The unfilled shell easily traps an electron if possible, from either thermal ionization, compensation or optical excitation. These factors will be considered in the next section. All acceptors produce energy levels about 1 eV above the valence band in the sulfides and 0.6 eV above the valence band in the selenides.

### Compensation

Donor impurities, since they are near the conduction band, are thermally ionized at room temperature. Their one excess electron is free to move in the conduction band. This produces high electron conductivity in halogen doped crystals due to high free electron concentration.

Acceptors entering 1 eV above the valence band are not as easily thermally ionized, tending to be unionized at room temperature. Thus they contribute very little to conduction at room temperature.

When both donors and acceptors are present in the crystal, compensation occurs. That is, the electrons thermally freed from donor levels are trapped at acceptor sites, supplying the extra needed valence electron; i.e., filling the hole.

The effects of compensation are twofold. First, the conductivity is lowered. If $N_p$ donors and $N_a$ acceptors are present, then $N_a$ donors can be compensated and the number of uncompensated centers is then $N_p - N_a$. For equal concentration of donors and acceptors, all donor electrons are trapped at acceptor sites and the concentration of free electrons is low. In the uncompensated case Cu is essentially in the doubly ionized state, $Cu^{++}$, to supply the two valence electrons as for $Zn^{++}$,

$$(Cu^{+})^{-} \rightarrow (Cu^{++})^{\circ} + e.$$

Second, compensation supplies an extra electron to $Cu^{++}$ to form $Cu^{+}$. The $Cu^{+}$ ion has one fewer positive charge compared to the original site ($Zn^{++}$ or $Cd^{++}$) for which it substitutes, and is therefore negative with respect to the crystal site. For this reason it has been customary to use the notation $(Cu^{+})^{-}$.

## Self Compensation

If only acceptors are incorporated in II-VI compounds, self compensation tends to occur by production of anion vacancies. Hence in ZnS:Cu, or CdS:Cu, the Cu may be in the form

$Cu^+$ even though not compensated by donor impurities. Sulfur vacancies can act as donor centers, producing two free electrons per vacancy, and compensating two acceptors.

$$V_S^\circ \rightarrow V_S^{++} + 2e$$

## III. Optical Excitation

We now consider the optically excited electronic transitions which are possible in an impurity doped II-VI compound. Figure 1-2 shows the five transitions which will be discussed. Other cases such as exciton states will not be considered.

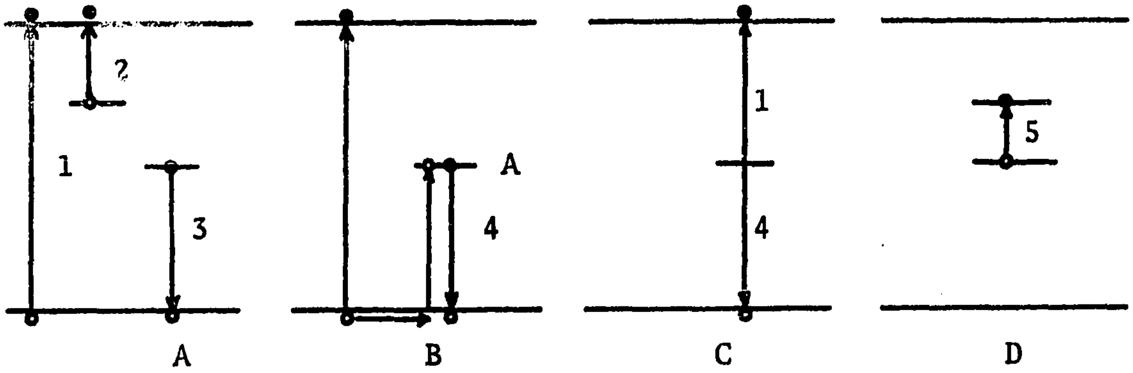

Figure 1-2. Optical excitation transitions.

1. Intrinsic excitation. For optical excitation whose energy is equal to or greater than the band gap energy, absorption may excite an electron from the valence band into the conduction band, producing a free electron and hole. This is called intrinsic excitation, and is characteristic of the material, not of any impurity. Intrinsic absorption of photons is very strong, with absorption coefficients above $10^5$/cm.

2. Extrinsic excitation. When impurity levels are

present in the forbidden band, an electron may be excited from that level to the conduction band, either optically or thermally. This is the case for donor centers such as a halogen, and also for compensated acceptor levels such as $Cu^+$,

$$(Cu^+)^- \rightarrow (Cu^{++})^\circ + e \text{ (cond. band).}$$

Here the hole is left in the center.

3. Uncompensated acceptors. It is possible to excite an electron from the valence band into the deficient acceptor center, leaving a hole in the valence band. This is generally referred to as excitation of a hole from the acceptor center to the valence band. In the case of ZnS and CdS the acceptor levels are deep and not thermally excited at room temperature,

$$Cu^{++} \rightarrow Cu^+ + h \text{ (valence band).}$$

4. Excitation of trapped carriers. Similar to ordinary extrinsic excitation, electrons and holes trapped at a center may be re-excited into the conduction band or valence band. The difference here is that previous excitation is necessary. A simple example of this is shown in Figure 1-2B. Primary band gap excitation, creating electron hole pairs, allows filling of a trap level A. Under this condition a new absorption and excitation is possible from A back to the valence band. Figure 1-2C shows a similar process using extrinsic primary excitation, producing a hole in the center directly. In both cases previous excitation is necessary.

5. Internal excitation. Many impurity centers such as Mn in ZnS show transitions between the ground state and an excited state of the center well within the band gap, so that

the transitions are confined to the center, and have no connection with the conduction or valence band, as in Figure 1-2D.

## IV. Electron Beam Excitation

Electron-hole pairs may be produced by electron beam excitation, the results being comparable to intrinsic optical excitation. However, optical excitation with band gap radiation produces one electron hole pair per photon whereas a high energy electron produces a shower of electron-hole pairs, many of which have high energy. Thus the process of electron excitation is of a more complex nature than optical excitation, and one must make sure that comparable results occur with the two methods. Electron beam excited luminescence is known to produce the same bands as optical excitation (1); the relative intensity of the separate bands is shifted, emphasizing the higher energy bands and the peak energy of each band may shift slightly to higher energies. However, for the purposes of the experiments performed, the two methods of excitation will be considered to be equivalent.

### Penetration Depth

Experimentally a 10 KV accelerating voltage was used to produce luminescence excitation. The depth of penetration for electrons of this energy have been variously reported to be between 1μ and 2μ (12). This is sufficient to be considered bulk excitation as compared to surface excitation since it extends at least a few thousand lattice constants into the crystal.

## Damage

The threshold for electron damage is well above the energies used. In ZnS, the threshold is reported to be about 200 KV (1).

# CHAPTER II

# LUMINESCENCE

Visible luminescence and phosphorescence have been known for ages, zinc sulfide being a main point of interest due to the availability of strongly luminescent natural samples. In the last forty years, ZnS has seen wide industrial application because of its high efficiency, and has been used in mass production of cathode ray tube screens, fluorescent lamps, and television tubes. This has stimulated considerable research on the production and properties of ZnS. Other II-VI compounds such as CdS have seen less emphasis since either their luminescence bands are in the red or infrared or that the compounds are more difficult to prepare.

Most studies of luminescent materials have been done on powdered samples since they are more easily produced than single crystals and most industrial applications require powdered phosphors. The information that grew out of industrial production stressed the importance of small impurity concentrations, activators and coactivators, and the influence of fluxes in preparing good phosphors; but knowledge of the luminescence mechanisms and identity of luminescent centers has been small. Phosphor preparation was more of an art than science.

Recently (1960) single crystals of ZnS and CdS have been available and this has given impetus to the understanding of the luminescence mechanisms. Critical experiments such as polarization of luminescence have led to information on the nature of the responsible centers.

Roughly five different models have been proposed for the various types of luminescence. All of these have been applied to the green copper (G-Cu) luminescence in ZnS on the basis of specific experimental evidence. In general, however, no single experiment can unambiguously verify a given model, nor can any one model explain all experimental evidence. For this reason it is desirable to perform a variety of experiments on the same or similar samples in order to form a unified description of luminescence and photoconductivity mechanisms.

Luminescence can be a useful tool in examining minute impurity concentrations. For example, as little as $10^{-6}$Cu/ZnS can easily be detected by its green luminescence. Copper in ZnS is known to give five different luminescence bands, depending on Cu concentration, the relative concentration of compensating donors (called coactivators), and conditions of preparation, firing temperature, flux and ambient gas pressure. Van Gool (13) has summarized these conditions in convenient form. For equal concentrations of Cu and coactivator in the range of approximately $1 \times 10^{-6}$ to $4 \times 10^{-4}$ Cu/ZnS, the green copper band is produced. This luminescence and its analogous band in CdS at 1.02μ will be two of the major topics of this work. For Cu concentration higher than coactivator concentration a blue band occurs in addition to the green. For copper without coactivator a red luminescence is seen, and for high and equal concentrations of Cu and a group III coactivator, In, Ga, or Sc, red emissions appear which depend on the specific coactivator. Finally there is an infrared luminescence at $1.5\mu$ - $1.65\mu$ in ZnS and $1.6\mu$ in CdS which is also characteristic of copper and occurs with or without the presence of coactivator. The green and infrared copper luminescence in ZnS and their analogues in CdS, have been the subject of this study since they are unique to the copper impurity and are presumed to represent the most basic of Cu centers possible. They will be discussed in the next section.

## I. Luminescence in ZnS:Cu and CdS:Cu

### Green Copper Luminescence

As mentioned in the introduction to this chapter, ZnS shows the characteristic green luminescence for approximately equal concentrations of Cu and coactivator between $1 \times 10^{-6}$ and $4 \times 10^{-4}$ Cu/ZnS. Since it is independent of the specific coactivator, mode of excitation, and probably represents the simplest Cu center, it is the logical choice for the study of the properties of $Cu^+$ and $Cu^{++}$ in ZnS and CdS.

Optical excitation is produced with band gap (3.7 eV) or extrinsic (2.5 eV) radiation, indicating a $Cu^+$ level of 1.2 eV above the valence band, (Schon-Klasens model, see section II). Electron beam excitation produces the same luminescence, and the properties are essentially independent of method of excitation. High efficiencies are achieved in good phosphors, with decay times in the range of $10^{-4}$ to $10^{-5}$ seconds, with long lived components which give a long phosphorescence. Luminescence efficiency is roughly temperature independent up to a temperature of about 250°C, where thermal quenching occurs by thermal release of trapped carriers, reducing efficiency by competitive non-radiative processes.

In CdS:Cu the equivalent to G-Cu is at 1.02μ (1.22 eV)(14), and has the same properties as in ZnS. In mixed crystals of ZnCdS the green band shifts monotonically to lower energies along with band gap for increasing concentration of Cd. Similar bands in ZnS and CdS are produced by Ag and Au, at different energies but of equivalent nature (15).

### Infrared (I.R.-Cu) Luminescence

The i.r.-Cu luminescence was first reported by Dumbleton and Garlick in 1954 (16). The origin of this emission, however, was in doubt. More recently (1959) Apple and Prener (17) have definitely shown it to be due to Cu. In their study they characterized the dependence on Cu concentration, coactivator concentration and sulfur pressure during firing. The i.r.-Cu intensity varied linearly with Cu concentration up to about $10^{-4}$ Cu/ZnS and was relatively independent of the presence of coactivator or sulfur pressure.

Weakliem and McClure (1962) (18) discussed the crystal field splitting of $Cu^{++}$ in ZnS and CdS. Broser and Schulz (7) found excellent experimental agreement with Weakliem and McClure using high resolution absorption and emission spectroscopy at low temperatures. They were able to resolve the structure due to phonon interaction and interpret it by using known lattice vibration modes. This study confirms the identity of the i.r.-Cu center as a $Cu^{++}$ ion on a zinc site, and gives a good basis for the study of optical effects on this luminescence.

The i.r.-Cu luminescence is excited by band gap radiation and also by 0.7μ and 1.3μ bands (8) indicating that there is a close correlation between the excitation spectrum and the absorption spectrum seen by Broser and Schulz. Additionally, two types of ZnS:Cu samples were found; those which required simultaneous U.V. excitation for stimulation in the 0.7μ and 1.3μ bands, and a second group which did not require simultaneous band gap excitation. This indicated that the number of $Cu^{++}$ centers was being increased by the band gap radiation.

## Other Luminescence Bands

As summarized by Curie, the three other luminescence bands due to copper in ZnS and CdS are attributed to more complex centers involving substitutional and interstitial Cu atoms. They are listed below for completion:

1. Blue Cu: Occurs when Cu is incorporated in excess of coactivator.
2. Red Cu: Produced by addition of Cu only.
3. Red Cu-In: For high Cu concentration with equally

high concentration of a IIIB coactivator.

4. Blue self-activated: Not due to Cu; produced by incorporation of coactivator only.

These bands have been well documented by Shionoya (19) and the assignment of the responsible center has been fairly well established. These bands will not be discussed further, they are listed to point out the range and complexity of the luminescence centers in ZnS and CdS.

## II. Luminescence Models

The earliest model for the G-Cu luminescence was proposed more than twenty-five years ago (Schon-Klasens, 1942) (20), but of the four fundamentally different models which have been proposed, there is still disagreement as to the suitable model for G-Cu luminescence. Effectively, the disagreement lies between the Schon-Klasens and the unassociated pair models. The various models will be presented in this section along with examples of supporting and conflicting evidence for each one.

### Schon-Klasens Model

The Schon-Klasens model, Figure 2-1, is characterized by hole trapping at a compensated $Cu^+$ center followed by radiative recombination with an electron in the conduction band. Since the other models may be developed as modifications of this basic form, we will follow the step-by-step process in some detail.

1. Excitation. An electron is excited from the valence band to the conduction band by optical or other means,

yielding an electron-hole pair.

2. Hole migration. The hole in the valence band migrates into the vicinity of a compensated acceptor ($Cu^+$).

3. Trapping. Since $Cu^+$ is substitutional for $Zn^{++}$, it appears as a negatively charged trap and has a large capture cross section for holes. The holes generally have a short lifetime in the valence band, about $10^{-8}$ seconds in a crystal with such traps. Note that after trapping, the center $Cu^{++}$ is neutral with respect to the crystal,

$$(Cu^+)^- = h \rightarrow (Cu^{++})^\circ$$

where the charge signs outside the brackets denote the charge of the center with respect to the rest of the crystal. As in photo-sensitization, the subsequent capture cross-section for electrons is small due to the neutrality of the center.

4. Electron migration. Concurrent with steps 2 and 3, electrons migrate into the vicinity of a trapped hole.

5. Radiative recombination. The electron in the conduction band radiatively recombines with the hole trapped at a $Cu^{++}$ center,

$$(Cu^{++})^\circ + e^- \rightarrow (Cu^+)^- + h\nu \ (2.35 \text{ eV}),$$

which returns the Cu center to its original state.

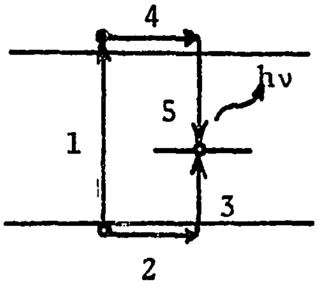

Figure 2-1. Schon-Klasens model.

There are many arguments in favor of the Schon-Klasens model and it has been largely accepted as the model appropriate to G-Cu luminescence. More recent experiments cast some doubt on this, however. Some of the arguments for the Schon-Klasens model will be given below, whereas conflicting data will be discussed with the other models.

1. Hall sign. The majority carriers are always found to be electrons in ZnS and CdS. A model where holes are quickly trapped by centers with a large hole cross section is most feasible.

2. Photoconductivity. The similarity between photoconductivity and luminescence excitation spectrum strongly indicates that the luminescence mechanism involves free carriers.

3. Coactivator dependence. The green-Cu peak energy does not depend on the specific coactivator, hence it is presumed that the coactivator does not enter into the luminescence process directly, but merely maintains charge neutrality in the crystal.

4. Temperature dependence. The fact that luminescence efficiency is essentially flat with temperature over a broad range suggests that the green-Cu transition is not from shallow donor levels, which would be affected by thermal excitation.

Contradictory evidence, based on the peak shift with time after excitation, is difficult to explain with the Schon-Klasens model. This will be discussed along with the unassociated pair model.

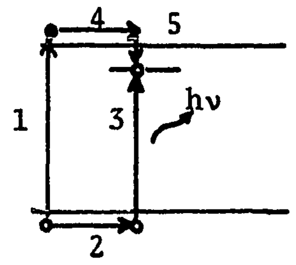

1. Intrinsic excitation
2,3. Hole migration and trapping by $\mathrm{Cu}^{++}$ center giving radiation
4,5. Electron migration and trapping by $\mathrm{Cu}^{++}$ center

Figure 2-2. Lambe-Klick model.

### Lambe-Klick Model

The Lambe-Klick (21) model is effectively the Schön-Klasens model with the roles of electrons and holes, donors and acceptors reversed. The Cu level is here assumed to be 1.2 eV below the conduction band, with the radiative transition occurring prior to electron migration and trapping. This is supported by the fact that the lifetime of photoconductivity is longer than that of luminescence. A major objection to this model is that extrinsic radiation at 2.8 eV is known to produce electron conduction, which would require a center 2.8 eV below the conduction band. This model has been used to explain the photoconductivity and luminescence decay times but is generally not considered applicable for G-Cu luminescence.

### Williams-Prener Model

In the Williams-Prener (22) or two level associated pair model, the Coulomb attraction between charged donors and acceptors is assumed to produce associated pairs during crystal growth, in excess of the normal random distribution of associated pairs, and that these are the luminescent centers. The electron transition is assumed to occur from the ground state or excited state of the donor and not from the conduction band.

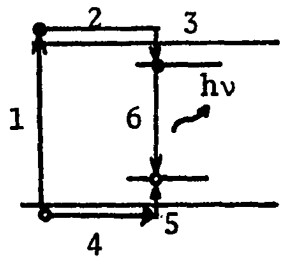

1. Excitation producing electron hole pairs.
2,3. Migration and trapping of electrons at donor centers.
4,5. Migration and trapping of holes at acceptor centers.
6. Radiative recombination between electron and hole at donor and acceptor pair sites.

Figure 2-3. Williams-Prener or two level associated pair model.

Two examples of conflicting evidence against this model are:

1. Coactivators in ZnS are known to produce shallow donor states 0.25 to 0.5 eV below the conduction band. These should be temperature dependent and therefore thermally ionized at room temperature, which should reduce luminescence efficiency due to the presence of competing non-radiative processes.

2. As mentioned, the G-Cu peak is independent of the specific coactivator; if transition were from the ground state there would be a detectable shift due to different coactivators.

### Unassociated Pair Model

Thomas and Hopfield (23) suggested that radiative

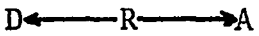

Figure 2-4. Unassociated pair model, interatomic distance R between unassociated donor and acceptor pair.

transition takes place between relatively distant donor-acceptor pairs. The transition probability W(R) and the radiated energy depend on the separation R, Figure 2-4, as

$$E(R) = E_g - (E_A+E_D) + \frac{e^2}{KR}$$

and

$$W(R) = W_o \exp\left(\frac{-R}{R_B/2}\right)$$

where E(R) = transition energy, $E_g$ = band gap energy, $E_A$ = energy level of acceptor, $E_D$ = energy level of donor, and K = static dielectric constant, $W_o$ = constant, $R_B$ = Bohr radius. E(R) decreases with increasing separation due to the last term $\frac{e^2}{KR}$ which is due to the core interaction. The donor and acceptor levels are pushed toward the band edges due to their interaction.

Evidence for donor-acceptor pair emission in GaP has been shown by Thomas and Hopfield. They observed a number of sharp lines corresponding to the different donor-acceptor pair distances. Also, the decay kinetics were examined, where a shift from higher to lower energy lines with time after excitation was found, in agreement with the transition probability W(R).

Studies by Shionoya, et al (4,5) show a definite spectrum shift of the G-Cu luminescence in ZnS with time after excitation and a shift to higher energy with increase in excitation energy. This is to be expected of donor-acceptor pair emission since at high excitation density the longer life pairs (greater R) will become relatively less important due to saturation. This presents strong evidence that the unassociated pair model may be applied to the G-Cu luminescence even though a sharp line spectra is not seen. Since the acceptor levels in ZnS and CdS are deeper than GaP, indicating stronger phonon coupling, the line spectrum may be obscured by broadening. Several arguments against this model that still exist are: 1. The efficiency is temperature independent. 2. The energy peak is not a function of the coactivator. 3. The energy peak is independent of the concentration. (24)

## III. Non-Radiative Recombination

Non-radiative recombination processes, which compete with luminescent transitions, lower the overall efficiency of luminescence. These centers, known as "killers," can be produced by the incorporation of deep acceptors such as Fe, Ni, or Co. Apparently these centers are strongly coupled to lattice vibration and are capable of dissipating several electron-volts of energy in the form of low energy phonons. How the center can convert several electron-volts of energy to many milli-electron-volt phonons is not clear. By way of example of the effect of killer centers, an Fe concentration of as little as $10^{-6}$ Fe/ZnS can affect the luminescent efficiency of ZnS:Cu.

Such killer centers will have an effect on any process which alters the carrier concentration, such as infrared excitation of trapped holes at $Cu^{++}$centers into the valence band. They compete for free carriers, including those re-excited by infrared. Hence some of those which had been trapped and destined for luminescence will be lost through the non-radiative processes. Thus, the presence of non-radiative centers is essential for the observation of infrared quenching of luminescence. Samples with low trap density are reported to show very little quenching sensitivity (25).

## IV. Effects of Infrared Radiation on Luminescence

Radiation in the 0.7μ to 2μ is known to have several effects on the luminescence of ZnS:Cu and CdS:Cu. Flash stimulation and long-term quenching of the G-Cu luminescence have been reported by many workers (26). The process involves re-excitation of trapped carriers into their band and provides a useful method for examining the energy levels of impurities, temperature dependence, and the complete description of the mechanism of luminescence. The various effects will be discussed in some detail.

### Flash Stimulation and Long Term Quenching

Considering the unassociated pair model, i.r. stimulation of trapped holes into the valence band redistributes the holes, thus increasing the importance of the faster centers (those with small donor-acceptor pair distance). This may be visualized by noting that the slow centers (large R) have a greater chance of losing a hole, since re-excitation probability depends on the product of excitation intensity and the length of time between capture and radiative recombination. Hence, the fast radiative centers and non-radiative centers become more important. This process causes the well known "flash" stimulation of the green, and the long term quenching.

The flash stimulation is independent of the presence of non-radiative centers, and depends on the jump in valence band hole density at the onset of i.r. radiation. Note that flash stimulation could be produced by hole excitation from any long life trap, not necessarily $Cu^{++}$, but the similarity of flash stimulation and quenching indicate that the majority of stimulation is from $Cu^{++}$ or centers with identical energy within the band gap. Quenching depends on the presence of non-radiative processes, and may not be seen in high quality samples. The net decrease in luminescence efficiency again depends on the fact that the non-radiative centers have a greater chance for hole trapping with i.r. present. The comparison of the i.r. luminescence excitation spectrum with flash stimulation and quenching of G-Cu luminescence indicate that the i.r. excitation is definitely due to Cu and not other centers.

## V. Thermal Quenching and Thermal Activation

Similar to infrared radiation, thermal energy may re-excite trapped carriers into the valence or conduction band. These effects become pronounced when the thermal escape probability exceeds the radiative transition probability.

## Thermal Quenching

At sufficiently high temperatures, approximately 250°C for ZnS, thermal excitation reduces the lifetime of the trapped carrier to such an extent that efficiency drops to a few per cent of the maximum. Considering an average radiative transition lifetime of approximately 5μs, quenching due to thermal excitation occurs when the lifetime for thermal transition drops below 5μs. Thermal quenching has not directly entered into consideration for this work, however its relation to thermal activation of optical quenching requires some discussion.

## Thermal Activation of Optical Quenching

It is noted that the 1.3μ quenching peak in ZnS:Cu is usually seen only at room temperature. The explanation for this involves thermal activation from an excited level. Optical excitation produces the transition to an excited hole state and thermal excitation excites the hole on into the valence band, Figure 2-5. As in thermal quenching, thermal activation will occur when the lifetime for thermal excitation becomes comparable to the lifetime in the level due to other processes,

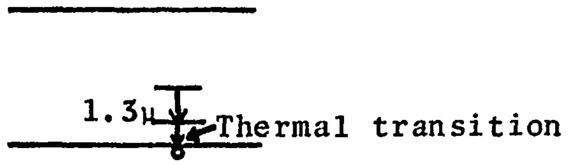

Figure 2-5. Thermal activation of optical quenching.

in this case, re-radiation back to the ground state. In ZnS:Cu, the excited $Cu^{++}$ level is about 0.5 eV above the valence band, and thermal activation should occur at about 200°K using the approximation of Uhrbach (22),

$$E(eV) = \frac{T°K}{400}.$$

## Two Step Optical Quenching

It should be possible to replace the thermal activation by optical excitation, Figure 2-6. This requires simultaneous excitation at low temperatures in two bands, one for the internal transition and the other for replacement of thermal activation. This has been shown for ZnS:Cu and will be discussed further in the data section.

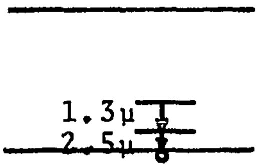

Figure 2-6. Two step optical quenching.

# CHAPTER III

## PHOTOCONDUCTIVITY AND MOBILITY

Photoconductivity in II-VI compounds has seen major research and industrial interest in only the last 20 years. This interest has been confined largely to CdS and CdSe although it is assumed that high photosensitivity can be achieved in all the II-VI compounds. Research on single crystals has been limited by the availability of samples of high quality. The history of preparation of single crystals of CdS dates back to 1946 with Frerichs preparation of CdS single crystals (27).

Photosensitivity in CdS and CdSe are the highest known to date of any photoconductive materials. Photoconductive quantum gains (electrons delivered to an external circuit per photon absorbed) are often as high as $10^5$ and $10^6$, and light to dark resistance ratios can be as high as $10^6$. Also, their spectral response falls in the visible and near infrared, making their possible uses infinite. These properties have stimulated much industrial as well as academic interest.

As in luminescence, small concentrations of impurities control the conductive and photoconductive processes of the II-VI compounds. Impurities can be incorporated to alter or control the photoconductive properties, spectral response, decay time, sensitivity; and conversely these properties can be used to study the characteristics of impurities in the host lattice. The energy levels associated with donor and acceptor impurities can be deduced by photoexcitation and i.r. photoquenching experiments. Also the mobility, sign, and lifetimes of free carriers can be studied by Hall mobility measurements. Comparisons to luminescence effects may be used to clarify the mechanism of luminescence. For example, the occurrence or absence of photoconduction associated with luminescence excitation indicates whether the process involves free carrier recombination or internal transition between excited states of the impurity.

The next section deals with those photoconductive properties of ZnS, CdS, and CdSe which are relevant to the optical quenching experiment and luminescence quenching. This requires discussion on the phenomenon of sensitization, superlinearity, carrier lifetime and carrier mobility.

## I. Photoconductivity

The conductivity of a material $\sigma$, is given by

$$\sigma = ne\mu_e + pe\mu_h$$

where n and p are the concentration of free charge carriers, electrons and holes respectively; e, the electronic charge, $\mu_e$ and $\mu_h$ the electron and hole mobility. The free carrier concentration in the absence of optical excitation is dictated by thermal excitation of carriers from the valence band to the conduction band.

Optical excitation produces free electrons and holes in excess of the thermally excited concentration, producing a change in $\sigma$, or photoconduction. The magnitude of the optical effect depends on the lifetime and mobility of the free carriers. These factors will be discussed in conjunction with a simple photoconductive model, Figure 3-1.

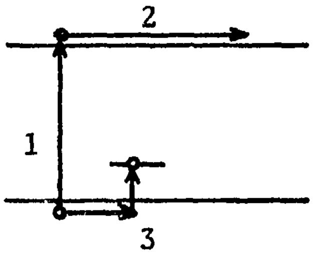

1. Optical band gap excitation produces electron-hole pairs.
2. Free charge carriers, mobile in cond. and valence band.
3. Trapping of one of the carriers.

Figure 3-1. Photoconductivity model.

For band gap optical excitation, free electrons and holes are produced in pairs, causing an increase in conductivity,

$$\Delta\sigma = \Delta n\mu_e e + \Delta p\mu_h e$$

where $\Delta n$, $\Delta p$ are the concentrations of free electrons and holes respectively, produced by photoexcitation. In this case we are neglecting the possible effects of a change in mobilities, $\mu_e$ and $\mu_h$, as a function of photoexcitation. This will be discussed later in connection with the Hall mobility. We denoted by the production rate g, the number of free carriers produced per unit time per unit volume. However the carrier concentrations $\Delta n$ and $\Delta p$, are not necessarily equal, since they depend upon the lifetimes $t_e$, $t_h$ of the free carrier as:

$$\Delta n = gt_e$$

$$\Delta p = gt_h \ .$$

This gives for the photoconductivity:

$$\Delta\sigma = gt_e\mu_e e + gt_h\mu_h e \ .$$

Since the mobility is largely characteristic of the material, and does not change appreciably, it is the electron and hole lifetimes which strongly control the photosensitivity. Lifetimes can range over many orders of magnitude in the same material, depending on impurity concentration. Often one carrier will predominate due to a much longer lifetime in photosensitive materials.

Free carrier lifetime is dependent upon trapping, recombination, and electrode effects. The conductive life of a photo-excited carrier is ended when any of these three effects takes it out of the conduction or valence band.

## Recombination

Recombination of electrons and holes usually occurs at some point defect center, with properties such that it has a large capture cross section for carriers of one type, followed by a large capture cross section for carriers of the other type, (Rose's Class I center) (28). The captured electron and hole recombine, either radiatively or non-radiatively. Normally produced pure CdS contains a high density of Class I centers which limit the electron and hole lifetimes to about 1 microsecond, and consequently having very low photosensitivity. The identity of these centers is not clear, but are probably shallow donor levels, possibly due to anion vacancies. These give high dark conductivity, due to thermal excitation, but negligible photosensitivity.

## Electrode Effects

If free carriers are replenished at one electrode as they leave the other, no effects on carrier lifetime will occur. This will be assumed to be the case under our conditions, a valid assumption because ohmic contacts are readily produced on CdS and CdSe. The reader is referred to the experimental section for a discussion on the preparation of ohmic contacts.

## Trapping

Charge carriers may be captured by centers called traps. These differ from recombination centers in that the probability for thermal re-excitation is larger than the probability for recombination. Thus the carrier is taken out of the conduction or valence band, held in the trap for some time, and then re-emitted by thermal excitation. The effect of trapping is to increase photoconductive response times in excess of normal carrier lifetime. As the electron Fermi level rises through a trapping level, the role of the center changes from trap to recombination center, i.e., it becomes more probable that the trapped electron will be lost due to recombination than due to thermal excitation. Thus the role of a center depends upon the conditions of optical excitation and temperature.

## Dark Conductivity

The addition of deep acceptor levels produces compensation of the shallow donors inherent in II-VI compounds, as discussed in Chapter II. The excess electron associated with the donor center is captured by the acceptor level as in Figure 3-2. This reduces the number of free electrons for conductivity, and the dark resistance is higher than for uncompensated samples. Copper is often added to CdS to increase the dark resistivity, serving as the deep acceptor level.

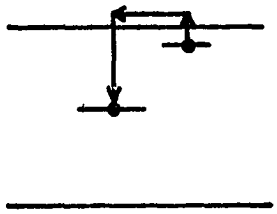

Figure 3-2. Compensation by deep acceptors.

### Sensitization

In the pure state, CdS and CdSe are not photosensitive, due to the high dark conductivity and short electron lifetime caused by the high density of shallow donor-recombination centers. The incorporation of compensated deep acceptor levels is necessary to produce highly sensitive materials. The process involved, called sensitization, changes majority carrier lifetime, dark conductivity, and reduces the minority carrier lifetime by trapping.

The properties of deep compensated acceptors which produce sensitization are large capture cross section for holes and small capture cross section for electrons after trapping a hole. These are essentially those conditions described by Rose as Class II centers. The effect of these centers is to capture photo-excited holes such that they are not available for recombination; their lifetime in the Class II centers is long compared to the free hole. This has two effects: 1. The lifetime of free electrons is greatly increased due to the decrease in the number of free holes available for capture by the efficient recombination centers, increasing the electron lifetime, and the photoconductivity. 2. The lifetime of free holes is greatly decreased due to the trapping effect of the Class II centers, and their contribution to conductivity is reduced.

This may be visualized in another way. The Class I recombination centers have a large cross section for electrons, and in the dark are empty due to compensation by the deep donors, thus limiting electron lifetime. In this condition the Class II deep acceptors are filled with electrons. Upon photo-excitation, holes are trapped by Class II centers and electrons by Class I centers. This effectively converts the deep acceptors to ineffective recombination centers. The free electrons now see filled donor levels and small cross section recombination centers, effectively changing the recombination traffic from Class I centers to Class II centers. This process can change the electron lifetime from about one microsecond in pure CdS to several milliseconds in sensitive CdS, a factor of up to $10^4$.

The identity of the deep acceptor-type centers is not required for a phenomonological picture of sensitive photoconduction, simply that it have the required properties of large hole capture cross section and subsequent small electron capture cross section. Possible centers with these properties are metal vacancies or compensated Group IB impurities. If Cu, for example, enters as $Cu^{++}$ and is compensated by shallow donors, it is singly positive in the dark: $Cu^{+}$. Since it substitutes for $Zn^{++}$ or $Cd^{++}$ it appears to have a net negative charge with respect to the crystal and will correspondingly have a small capture cross section for electrons,

$$[Cu^{+}]^{-} + h^{+} \rightarrow [Cu^{++}]^{\circ}\,.$$

The other possibility, a cation vacancy, can also act as a Class II center,

$$[V_c]^{--} + h^{+} \rightarrow [V_c^{+}]^{-}$$
$$[V_c^{+}]^{-} + h^{+} \rightarrow [V_c^{++}]^{\circ}\,.$$

Having captured two holes, the vacancy appears neutral to the crystal, and a correspondingly small capture cross section for electrons.

## Extrinsic Excitation

Electrons may be excited from impurity levels into the conduction band, producing extrinsic excitation. The holes are directly trapped at the impurity level, and are not mobile in the valence band.

This may be compared to extrinsic excitation of luminescence, and is seen to correspond to the Schon-Klasens model.

## Infrared Effects

The effects of infrared excitation of holes into the valence band on photoconductivity are twofold, causing photo-quenching and introduction of two carrier conductivity. Photo-quenching, as in luminescence quenching, is caused by the increased probability for electron-hole recombination when holes are in the valence band. During photo sensitization, holes are trapped, changing the Class II centers into weak recombination centers and redirecting the recombination traffic from Class I centers through the Class II centers. Quenching reverses this process, holes now being trapped and recombining again at the Class I centers. The majority carriers again see a high density of large cross section centers, which reduces their lifetime.

It is instructive to compare this to luminescence quenching, which requires the presence of non-radiative traps. The non-radiative traps compete with radiative transitions, thus quenching luminescence. In photoconductivity, however, we have made no assumptions about the presence of non-radiative traps; the only requirement being that holes recombine faster in the presence of i.r. than without it. This is possible if, as in the unassociated pair model, holes are being used by the faster luminescence centers under the i.r. radiation. In the case of a crystal with no non-radiative traps, one should be able to see photo-quenching without luminescence quenching. This is seen to be the case in many of the ZnS samples we have examined, the luminescence quenching being far smaller than the photo-quenching effects, indicating that non-radiative trap density is much smaller than luminescent center density.

One may recall that the electron mobility has been considered constant throughout this discussion. In fact, the change in mobility is much less than the change in electron lifetime. The electron mobility may change by a factor of the order of two due to the increased scattering effect of charged donor centers. However the change in lifetime may be several orders of magnitude, usually overriding the mobility effect.

## II. Hall Mobility

As we have seen, photoconductivity and the effects of a secondary radiation on photoconductivity can yield information about the mechanisms involved in optical excitation. It is possible to estimate the band gap energy, (intrinsic excitation edge), the impurity energy level within the band gap, by extrinsic photoconductivity and optical quenching. However, the latter information is ambiguous in the sense that the sign of the carriers is not uniquely defined, and the effect of secondary radiation can either be attributed to a change in carrier mobility or a change in carrier lifetime. The study of the Hall mobility allows us to eliminate these two ambiguities.

First, the sign of the majority carriers can be deduced from the sign of the Hall voltage. Since the Hall field depends on the sign of the carrier e,

$$E_y = -\frac{1}{ne} B_Z j_x,$$

where $B_Z$ is the magnetic field, $j_x$ is the current due to the applied field $E_x$. It is well known from Hall mobility experiments that ZnS, CdS, CdSe are always n-type semiconductors, due to the characteristic type I shallow donor levels which occur even in pure samples. It is not possible to overcome this n-type conductivity by the incorporation of acceptors since they enter as deep levels, and an excess of acceptors will be accompanied by self-compensation. Hence the hole conductivity cannot dominate.

The knowledge that we have n-type conductivity in the case of extrinsic photoconductivity immediately removes one ambiguity, the position of the impurity level in the band gap. Before, it was impossible to tell whether extrinsic radiation should be associated with the energy separation from the valence band or conduction band. Now in the case of ZnS, CdS, CdSe, it is known that the extrinsic photo-excitation energy must be associated with the separation of the energy level from the conduction band. In addition, this knowledge of the carrier sign suggests that the mechanism of optical quenching is related to the energy distance of the impurity level from the valence band. Hence the i.r. energy for quenching gives the height of the impurity level above the valence band.

Second, one must separate out the contribution of photoquenching by change in majority carrier lifetime, and majority carrier mobility, and the possible contribution to photoconductivity by minority carriers released by infrared. The photo-induced conductivity was seen to depend upon the sum of conductivities of electrons and holes,

$$\begin{aligned} \sigma_{\text{Total}} &= \sigma_e + \sigma_h \\ &= n\mu_e e + p\mu_h e \end{aligned}$$

$$\sigma_{Total} = g\tau_e\mu_e e + g\tau_h\mu_h e,$$

from the photoconductivity discussion. The Hall constant is given by (29),

$$R = \frac{p\mu_h^2 - n\mu_e^2}{e(p\mu_h + n\mu_e)^2},$$

and the Hall mobility,

$$\mu_H = \frac{p\mu_h^2 - n\mu_e^2}{p\mu_h + n\mu_e}.$$

Here we see that the Hall voltage is proportional to $\mu_H$,

$$E_{Hall} = \mu_H B_Z E_x,$$

and varies as the difference of the terms $p\mu_h^2$ and $n\mu_n^2$, and will equal zero when $p\mu_h^2 = n\mu_e^2$.

Thus, $\mu_H$ will decrease if the minority carrier contribution becomes appreciable, as may occur in infrared quenching of photoconductivity. Since normal conductivity in CdS and ZnS is n type, n<<p, we expect single carrier conductivity under primary excitation and two carrier conductivity during quenching.

## Single Carrier Conductivity

When carriers of one type dominate the conductivity, we have, for electrons,

$$\sigma = ne\mu_e,$$

and

$$\mu_H = \mu_e,$$

and since the Hall voltage is proportional to the Hall mobility, the Hall voltage will reflect only the electron mobility.

Generally the electron mobility will remain constant within a factor of two as a function of photo-excitation. This change is caused by the increase in charged scattering centers as the excitation raises the electron Fermi level. The case of constant mobility single carrier conductivity can be shown for ZnS and CdS over a range of photo-excitation. The changes that do occur are small compared to those produced by infrared initiation of two carrier conductivity.

## Two Carrier Effects

When both carrier types make appreciable contribution to the conductivity, as may be the case for infrared quenching, the Hall mobility is expected to drop as minority carrier concentration increases. This has been shown to be true in ZnS and CdS where the Hall mobility may be varied by a factor of 100 by secondary radiation.

# CHAPTER IV

## DATA AND RESULTS

Included in this chapter are luminescence and photoconductivity spectra, luminescence, photoconductivity and Hall mobility quenching spectra, and intensity and quenching intensity dependence. The data centers around the optical quenching of luminescence, photoconductivity, and mobility. The topics such as spectra, and intensity dependence take the form of supporting and corroborative evidence for the mechanism of luminescence quenching. Further, the photoconductivity and mobility data are presented in support of the luminescence data. Interpretation of the data are given in the body of the text.

### I. Green and Infrared Luminescence of ZnS:Cu:Cl

The ZnS:Cu:Cl samples used in this study were vapor grown single crystals containing 0.004 per cent and 0.04 per cent Cu per ZnS with Cl as the coactivator. The samples were supplied by the General Telephone Company (30). The physical appearance of the 0.04 per cent samples varied from clear green crystals to darker grey crystals. The 0.004 per cent samples were a uniform light green in color. Under band gap radiation, all showed a bright green or blue green luminescence at room temperature and 77°K. The spectrum for a typical crystal is seen in Figure 4-1; the luminescence is produced by electron beam excitation. The blue and green peaks are approximately the same intensity. The peaks are shifted toward the blue due to the spectral response of the 1P21 photomultiplier. Wide variation in the relative amplitude of the blue and green peaks is seen among crystals.

With optical or electron excitation, the two infrared peaks (i.r.-Cu) can be seen. Figure 4-2 shows the infrared spectrum using electron beam excitation. The luminescence intensity is low, resulting in considerable scatter in the monochromated spectrum, as indicated by the error bars. Accurate emission spectra for these samples have been done by C. R. Yarger of this laboratory (31). For excitation experiments, thin film filters (see Ch. V) are used in place of the monochromator, giving increased intensity.

The intensity of the i.r.-Cu luminescence was enhanced by redoping the available crystals with Cu and firing in a sulfur atmosphere. This increases the uncompensated Cu center concentration, the high sulfur pressure preventing self compensation. Although the final i.r. emission was still low, it was adequate for excitation experiments.

## II. Quenching and Stimulation of the Green ZnS:Cu Luminescence

It is well known that the G-Cu luminescence may be quenched by infrared radiation in the 0.7μ-0.8μ and 1.35μ regions (32). Also transient stimulation of G-Cu at low

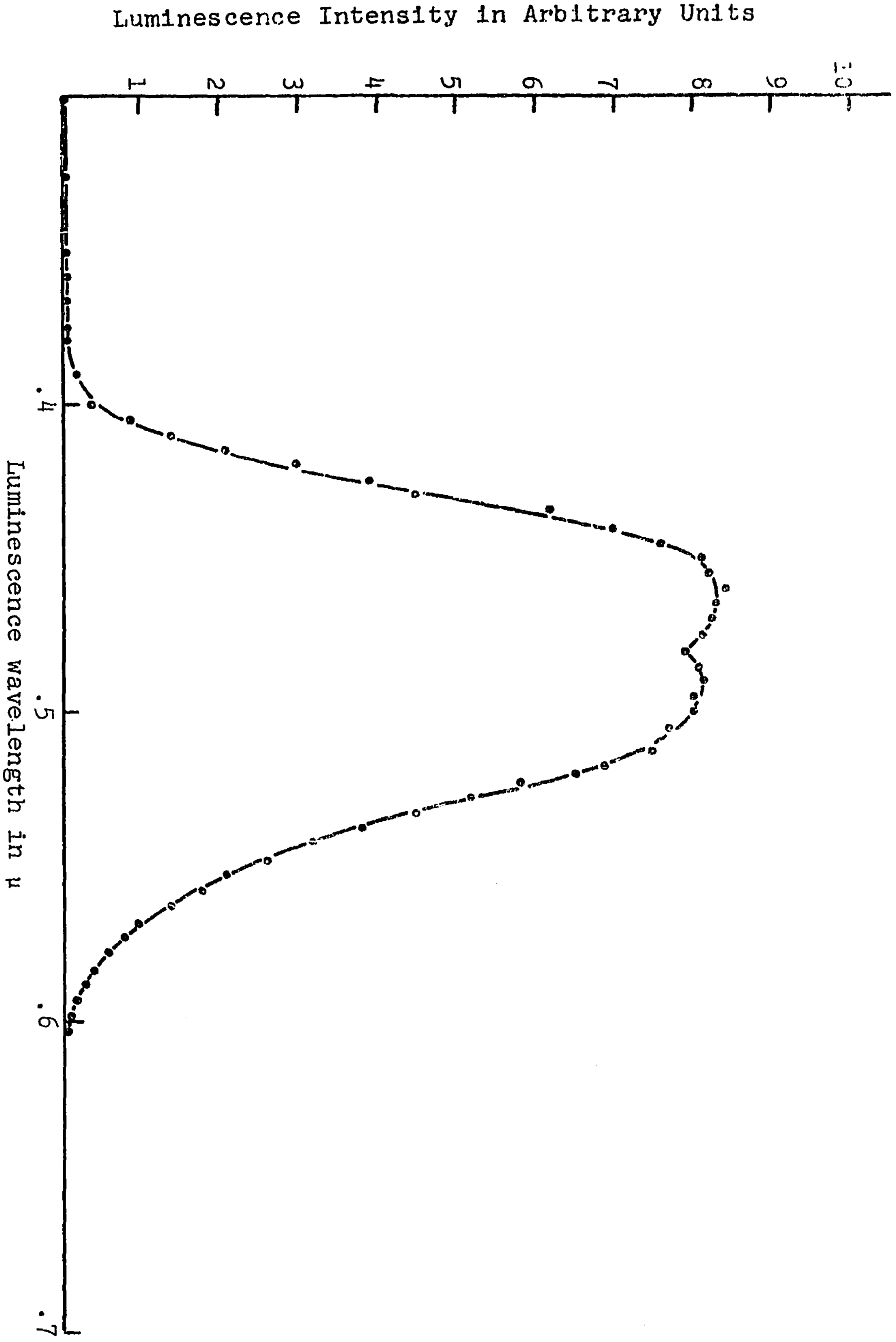

Figure 4-1. Visible luminescence spectrum of ZnS:Cu.

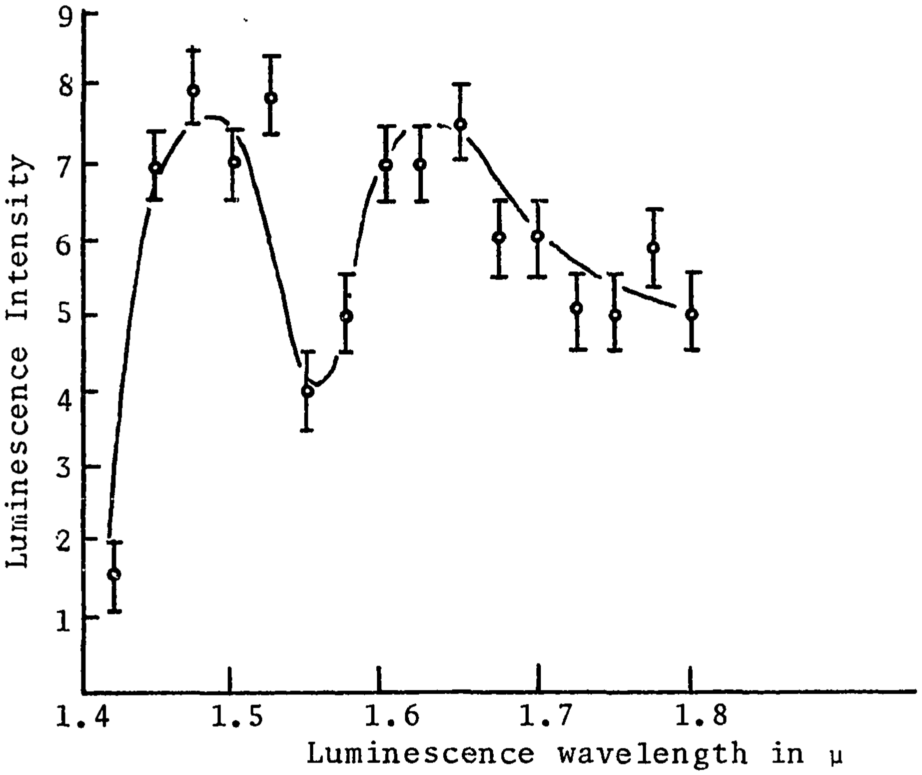

Figure 4-2. Infrared-Cu luminescence in ZnS:Cu.

temperatures has been reported at these same wavelengths (28). The quenching efficiency of the 1.3μ band has been seen to be temperature dependent, being smaller at low temperatures. The effects of infrared radiation on the steady state G-Cu luminescence intensity at 77°K and 300°K are shown in Figure 4-3 to 4-5. In these graphs the per cent quenching of the luminescence due to infrared radiation is plotted as a function of the quenching radiation,

$$\%Q(\lambda) = \frac{I_o - I_{IR}}{I_o}.$$

Where $I_o$ is the luminescence intensity produced by a constant primary (electron beam) excitation, and $I_{IR}$ is the luminescence intensity produced by the same primary excitation and simultaneous infrared radiation. The primary excitation is held constant throughout the experiment and various optical filters are used to select the secondary quenching radiation. In each case the i.r. radiation is normalized for constant intensity between the range of 0.8μ to 1.7μ. The 0.7μ filter was not normalized due to inadequate intensity. In Figure 4-3 the 0.7μ-0.8μ peak is roughly independent of temperature whereas the 1.3μ peak is considerably reduced at low temperatures, indicating the effect of thermal activation. Due to scattered light reaching the detector, the 0.5μ and 0.6μ points could not be measured.

Figure 4-4 shows quenching spectra for several different luminescence intensities $I_0$, which vary in relative magnitude from 1 to 1,000. The maximum quenching is seen to occur for the lowest luminescence levels. Relative luminescence intensities are indicated as 10, 100, and 1000 times the base intensity.

Figure 4-5 shows infrared quenching for a sample which had been redoped with Cu, and annealed at 800°C in a sulfur atmosphere; the quenching efficiency is greater in this case, and shows the same two peaks.

Discussion of error and standard deviation of data. The quenching data shown in Chapter IV shows typical spectral dependence that was seen in the experiment. The reproducibility of points for a given crystal was approximately 10 per cent, whereas there was extremely wide variation in quenching effects from sample to sample, ranging from no detectable quenching to about 80 per cent to 85 per cent.

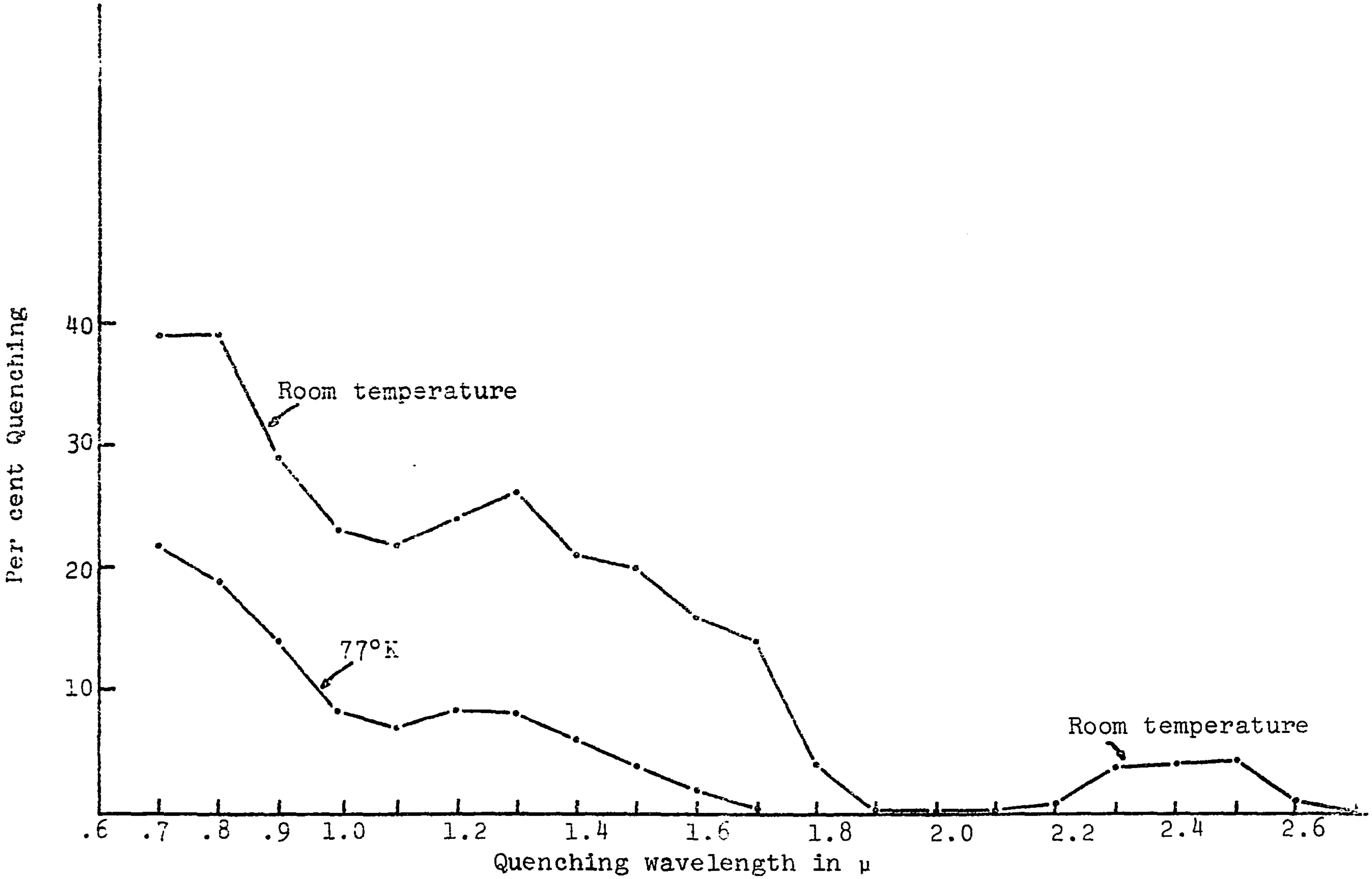

Figure 4-3. Quenching of G-Cu luminescence in ZnS:Cu.

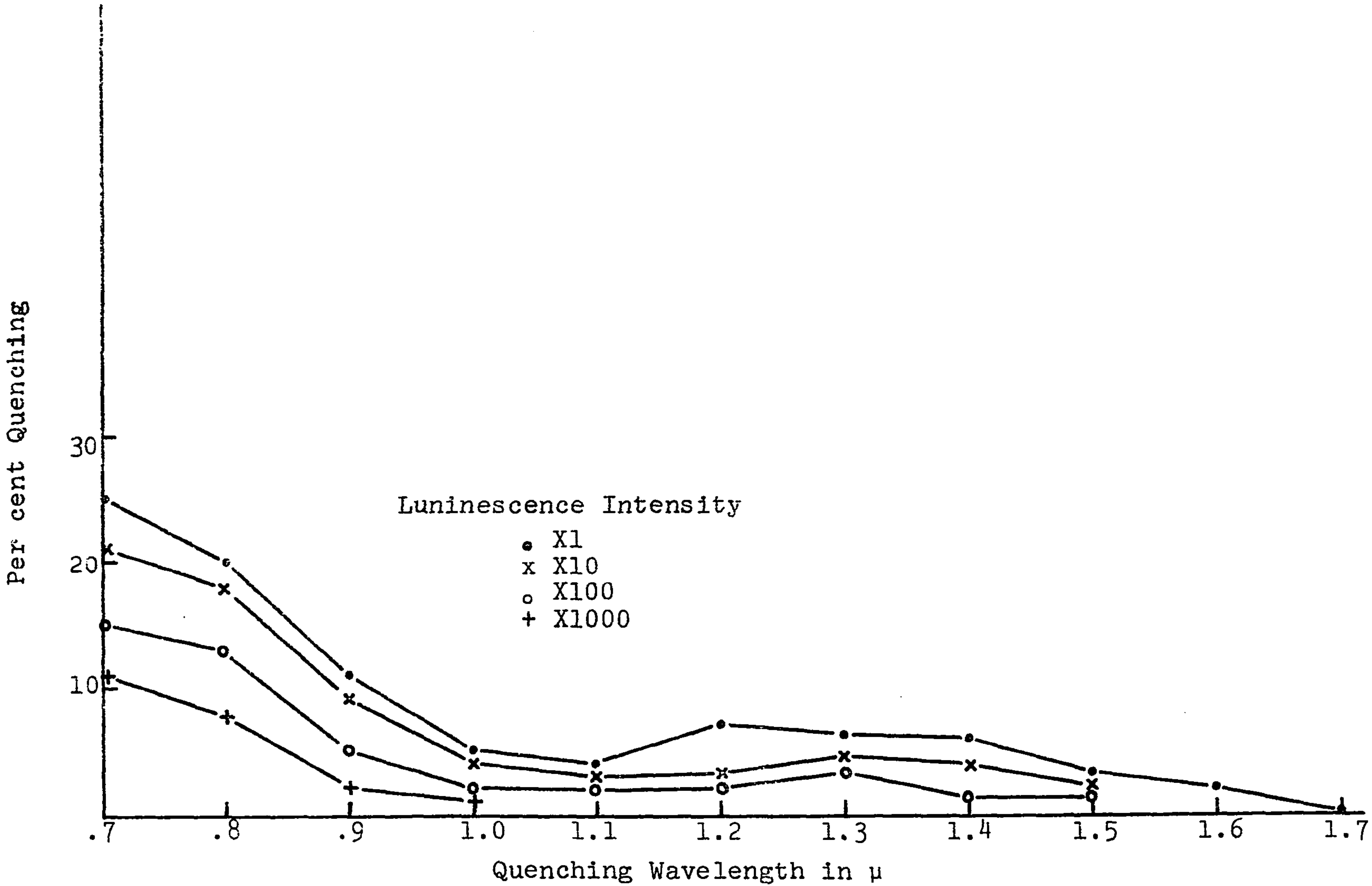

Figure 4-4. Quenching of G-Cu luminescence in ZnS:Cu at 77°K for various luminescence intensity.

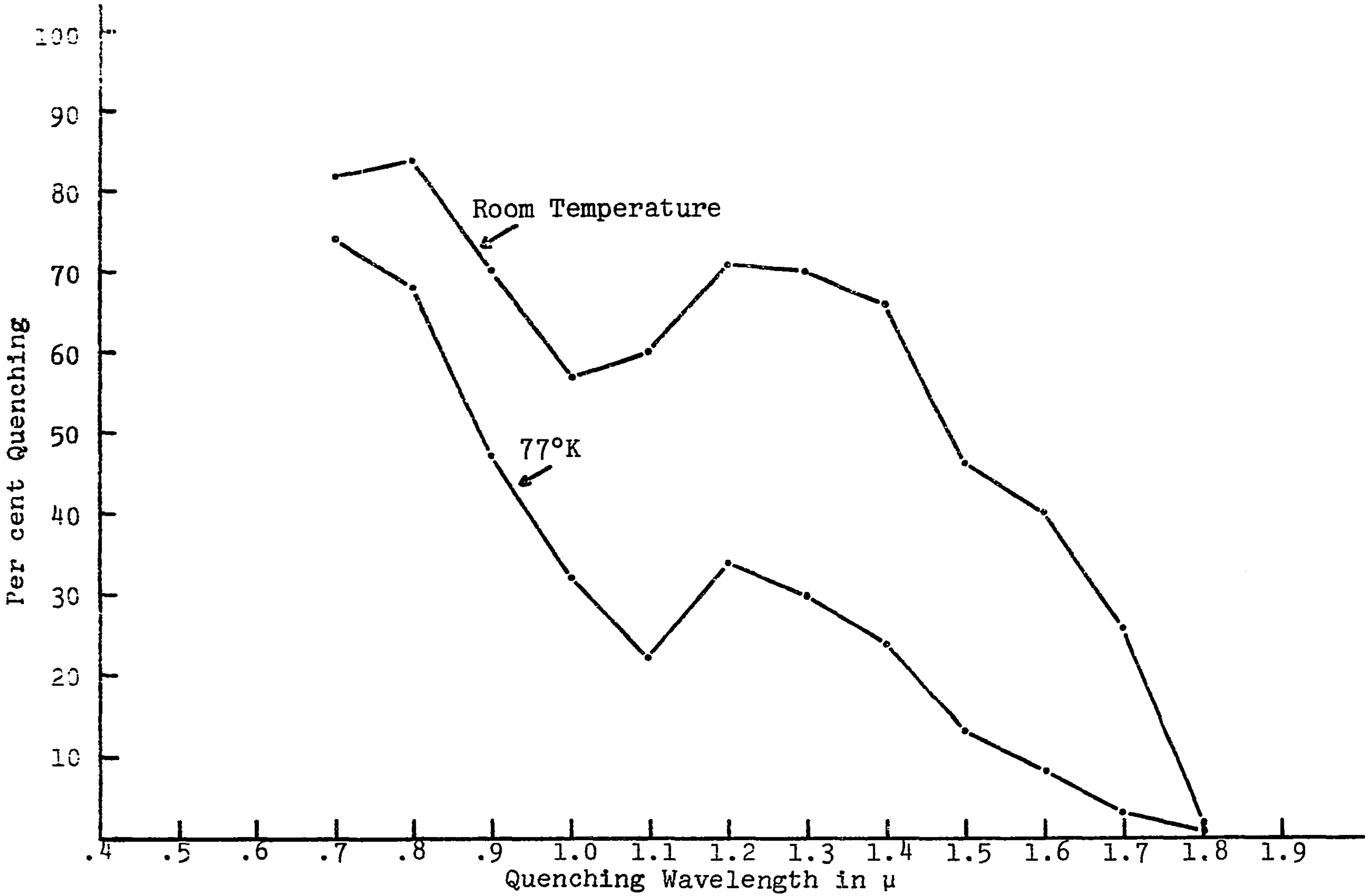

Figure 4-5. Quenching of G-Cu luminescence of ZnS:Cu, at room temperature and 77°K.

In each case the application of i.r. radiation produces a transient stimulation of the luminescence followed by the long term steady state quenching. The stimulation was especially apparent at 77°K. The stimulation spectrum followed the quenching efficiency spectrum closely. The similarity between the transient stimulation and the long term quenching has been previously noted (33). Some workers have interpreted the stimulation as due to a resonant energy transfer to trapped electrons, and others interpret it as a redistribution of holes to centers with higher electron capture cross section (34). It is possible, however, to explain the stimulation and quenching by the same mechanism following the unassociated pair description of Era, Shionoya, and Washizawa (Ch. II). According to these authors, luminescence arises from unassociated donor-acceptor pairs, the pairs with large atomic separation having small transition probability (slow centers) and those with small atomic separation having large transition probability (fast centers). The quenching radiation excites holes out of all the $Cu^{++}$ centers into the valence band. This, in effect, transfers holes from the slow centers to the fast centers, causing the initial rise in luminescence intensity. The presence of competing non-radiative traps then lowers the luminescence efficiency below the excitation-only condition, causing quenching. If there were no competitive processes, one would see only transient stimulation, the luminescence returning to its original level. Hence both stimulation and quenching are explained by the same process, stimulation due to the loss of holes from the slower centers, and quenching due to loss of holes to competing recombination. This seems to provide a more satisfactory explanation of the spectral resemblance of quenching and stimulation.

## III. Excitation of the I.R.-Cu Luminescence

The infrared emissions at 1.5μ and 1.65μ and absorption at 1.35μ have been identified by Broser et al, as the transition between the two levels resulting from the crystal-field splitting of the ground state of the $Cu^{++}$ ion in a tetrahedral field (7). It has been pointed out by several workers that the i.r.-Cu luminescence can be excited by 0.7μ and 1.3μ radiation (35). A typical excitation spectrum of i.r.-Cu is shown in Figure 4-6. The excitation spectrum was done in the same manner as the G-Cu quenching spectrum: The electron beam excitation produced a steady state luminescence, $I_0$, and the infrared radiation was added, increasing the i.r. luminescence. Two peaks are seen which correspond to the two quenching maxima for G-Cu. The two peaks are ascribed to the transition of holes from $Cu^{++}$ centers to the valence band and to the excited state of the level. Since the long wavelength peak of the excitation spectrum occurs at the same wavelength as the i.r. absorption, we may identify the hole excited state as the crystal-field level of $Cu^{++}$. The transient response is sketched in Figure 4-6b. The i.r.-Cu luminescence is seen to rise sharply with the application of i.r. and fall slowly to a level somewhat higher than the original intensity, $I_0$.

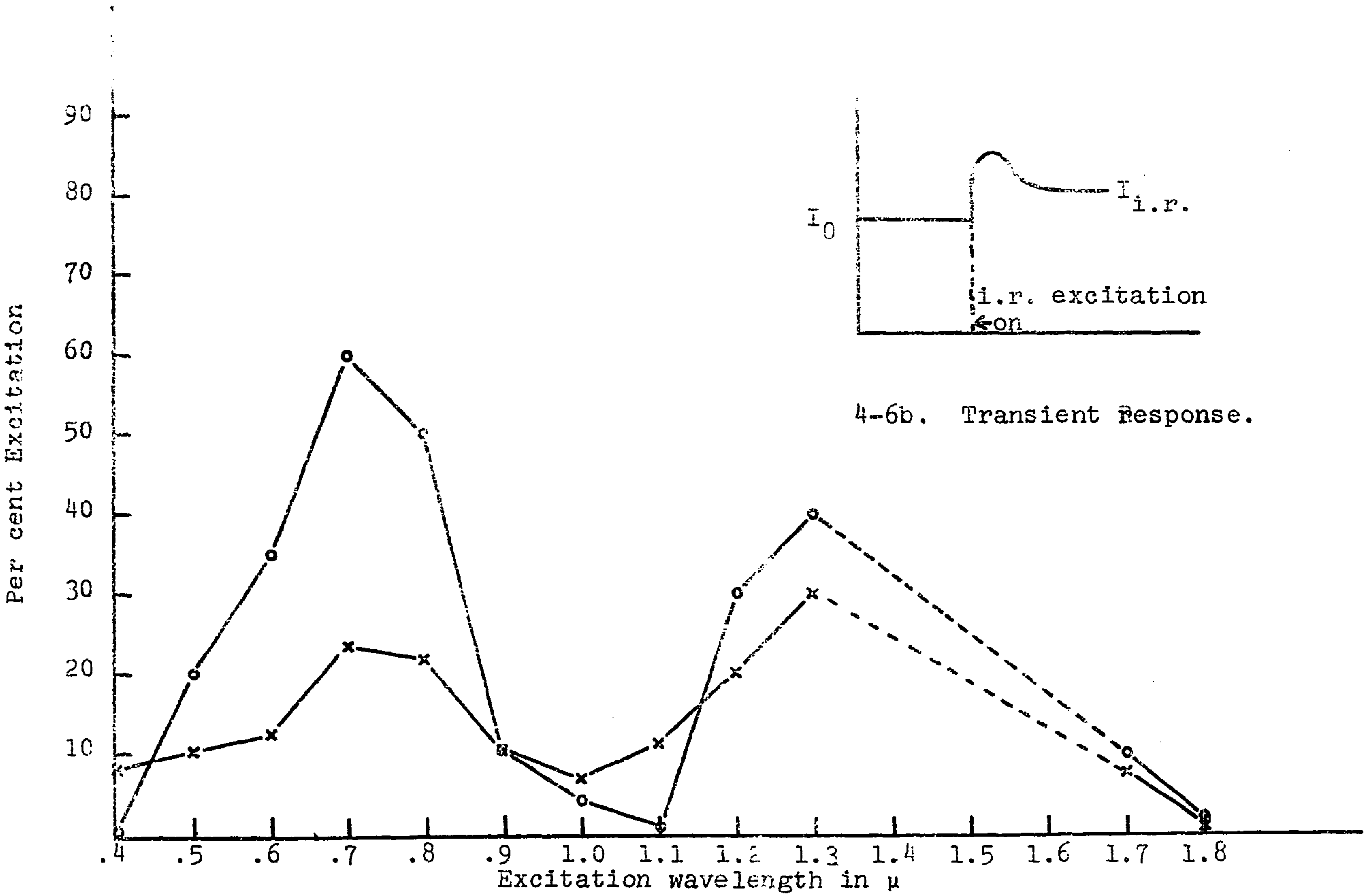

4-6b. Transient Response.

Figure 4-6. Excitation of i.r.-Cu luminescence of ZnS:Cu.

This is interpreted as stimulation due to transition of a hole from the $Cu^{++}$ ground state to the excited state, causing i.r. luminescence excitation in excess of the electron beam excitation. This is accompanied by quenching due to loss of $Cu^{++}$ concentration by competing processes, causing the intensity to fall slowly to level $I_{i.r.}$. Thus a composite result is seen in the final steady state intensity, showing the effects of excitation and quenching. It is assumed that if the quenching effect were more pronounced, the level $I_{i.r.}$ would fall below the initial level $I_0$. The distinction is made here in comparison to the transient stimulation of the G-Cu luminescence, that the i.r.-Cu excitation is constant, and the steady state level involves excitation and quenching , whereas for G-Cu quenching, no constant stimulation occurs due to i.r. radiation.

## Optical Excitation of I.R.-Cu Luminescence before and after U.V. Excitation

Two different types of ZnS have been reported regarding excitation of the i.r.-Cu luminescence. Both show optical excitation of the i.r.-Cu luminescence at 0.6μ-0.8μ and 1.3μ, but the one group requires simultaneous U.V. excitation whereas the other group is stimulated by the infrared alone (36).

Our samples were found to luminesce without U.V. excitation, but that U.V. excitation enhanced the intensity of the i.r.-Cu luminescence. The experiment was performed as follows: the sample was cooled to liquid nitrogen temperature without optical excitation. At liquid nitrogen temperature, two

0.6μ-0.8μ optical excitation spectra were run, one before and one after irradiation with U.V. Figure 4-7 shows the excitation spectrum in the 0.6μ-0.8μ region, showing an increase of a factor of 5 in luminescence intensity after U.V. irradiation.

The interpretation of this result is that there is some concentration of $Cu^{++}$ stable in the dark, probably uncompensated Cu. These are responsible for the small i.r. luminescence present without U.V. excitation. In addition, there must be a group of $Cu^{+}$ centers, which when optically excited at a liquid nitrogen temperature, have a long lifetime, giving rise to the larger i.r. luminescence. These centers are probably the isolated, compensated Cu centers, where the interatomic distance to the nearest coactivator is large, giving the center a long lifetime in the divalent state.

## IV. Quenching of the Green-Cu Luminescence by 2μ-3μ Radiation

According to the two level scheme of the $Cu^{++}$ center as shown in Figure 4-8, i.r. radiation corresponding to electron transition 3 will obstruct the holes in the $^2E$ level, and if sufficient thermal activation exists to excite holes from the $^2T$ to the $^2E$ level, optical quenching of G-Cu luminescence may again occur. To test this point we have examined the quenching spectrum between 2μ-3μ and found a small quenching peak from 2.3μ to 2.5μ, producing about 2-3 per cent quenching. In order to gauge the maximum possible quenching, a 2μ-3μ, broad band filter was used, giving about 5 per cent quenching at room

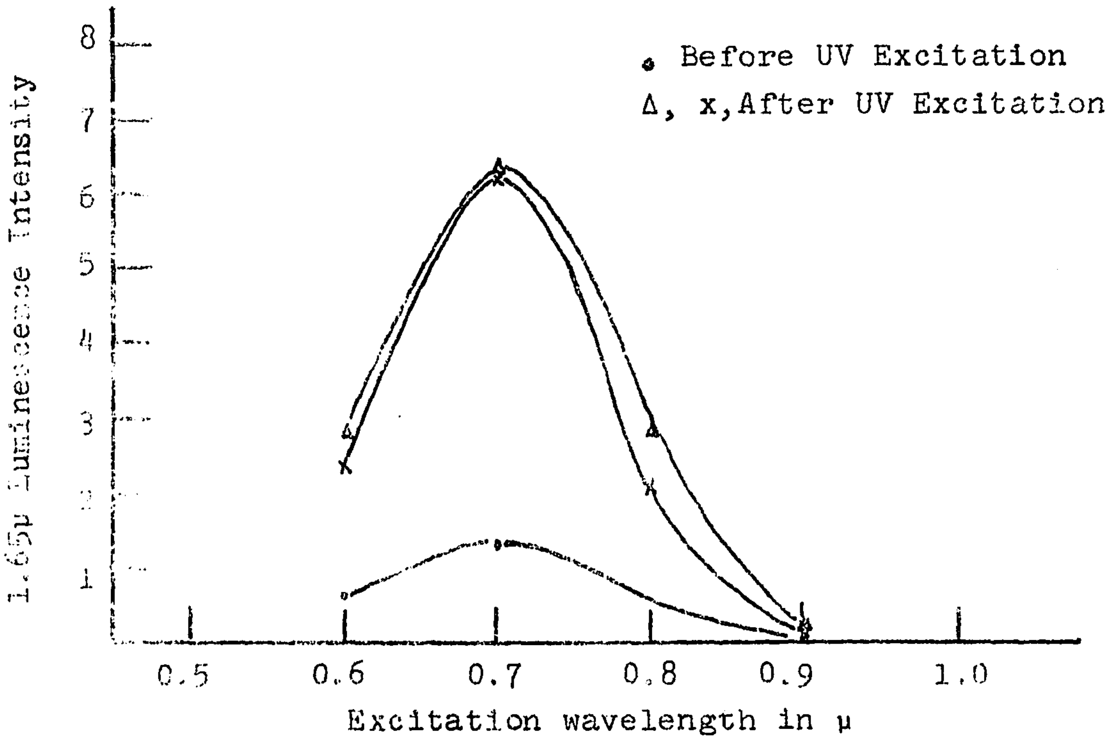

Figure 4-7. Optical excitation spectrum of i.r.-Cu luminescence, and dependence on pre-excitation by U.V.

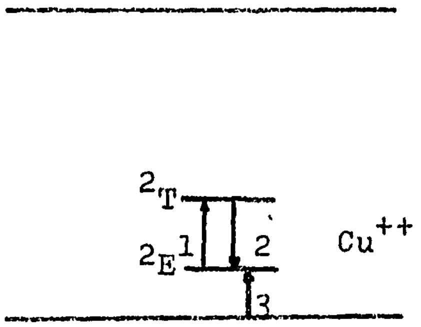

Figure 4-8. Energy diagram for $Cu^{++}$ in ZnS.

temperature and none at 77°K. This corresponds well to the proposed height of the $^2E$ level above the valence band, 0.5 eV, and corresponds to the normal thermal activation of the 1.3μ quenching peak. Also the fact that no 2.4μ quenching is seen at 77°K indicates that thermal activation is necessary, this time from the $^2T$ to the $^2E$ level. Initial stimulation was also observed in association with this quenching.

A stimulation band at 2.6μ has been previously identified as due to electron release from 0.5 eV electron traps. Using the Urbach formula for the temperature of maximum thermoluminescence as an indication of the temperature at which thermal activation becomes efficient, we get about 90°C. This is in agreement that the 2.4μ quenching is not seen at 77°K.

Since both the 2.6μ and 1.3μ quenching of the G-Cu luminescence require thermal activation, it should be possible to use a two step optical excitation process at low temperature where thermal activation is not effective. We conducted such an experiment on ZnS:Cu by irradiating it simultaneously with 1.3μ and 2μ-3μ radiation at 77°K. The 1.3μ alone produced about 9 per cent quenching and 2μ-3μ alone produced no quenching at all. However the combination of the two produce about 12 per cent quenching, an increase of about 3 per cent. These results support the assignment of the 2.5μ radiation to hole transition from the lower $Cu^{++}$ level to the valence band.

## V. CdS:Cu Luminescence

Similar results are found for CdS:Cu luminescence quenching as for ZnS. The counterpart of the G-Cu luminescence of ZnS lies at 1.0μ in CdS, falling between the two quenching peaks. This presents greater difficulty for the isolation of the quenching radiation from the detector.

The luminescence emission spectrum for two different samples is shown in Figure 4-9,10. This points out the variety in spectral emission of different samples. The 0.8μ peak corresponds to the blue copper ZnS luminescence and the 1.0μ peak to G-Cu.

The 1.0μ luminescence quenching spectrum for CdS is shown in Figure 4-11. The 0.8μ and 1.3μ-1.4μ peaks are seen. The 1.0μ point is missing, due to interference with the detection signal.

## VI. Photoconductivity and Photo Hall Mobility

Since the two quenching peaks of luminescence of both ZnS:Cu and CdS:Cu are associated with ejection of holes to the valence band, one may expect to observe a change in the Hall mobility under infrared quenching, as a result of hole conduction. When both electrons and holes make appreciable contribution to electronic conduction, the conductivity and Hall mobility ($\mu_H$) are related to the concentrations and mobilities of electrons and holes, as discussed in Chapter III,

$$\sigma = pe\mu_h = ne\mu_e$$

$$\mu_H = (p\mu_h^2 - n\mu_e^2)/(p\mu_h + n\mu_e)$$

For the case of single carrier electron conduction the Hall mobility should be independent of the carrier density or

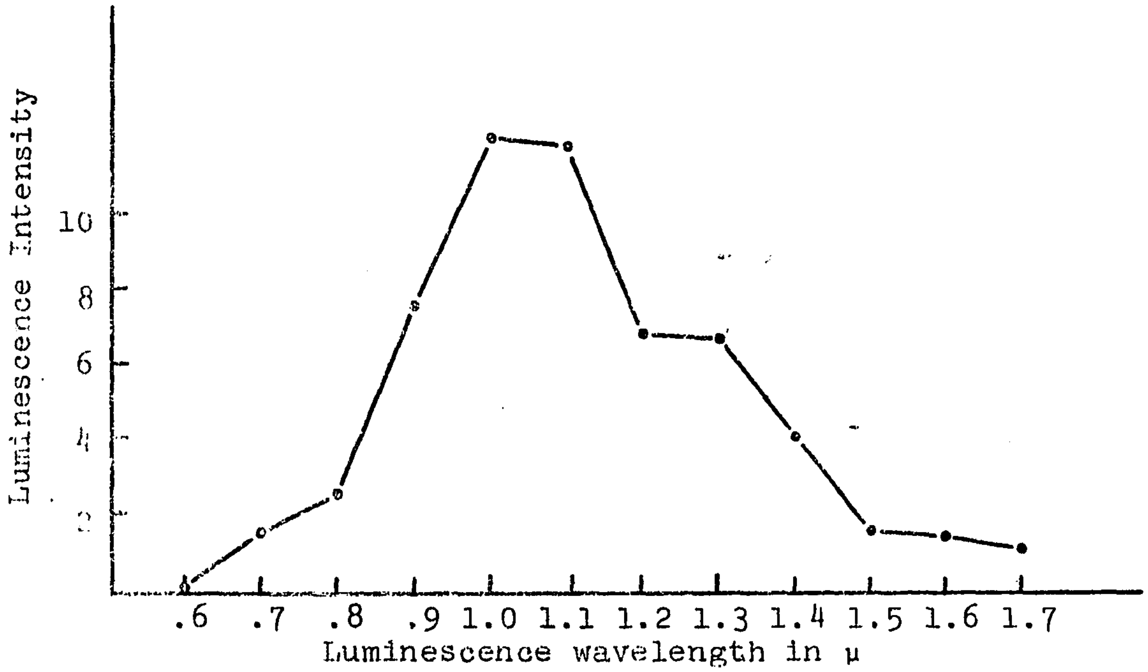

Figure 4-9. Luminescence spectrum of CdS:Cu:Cl.

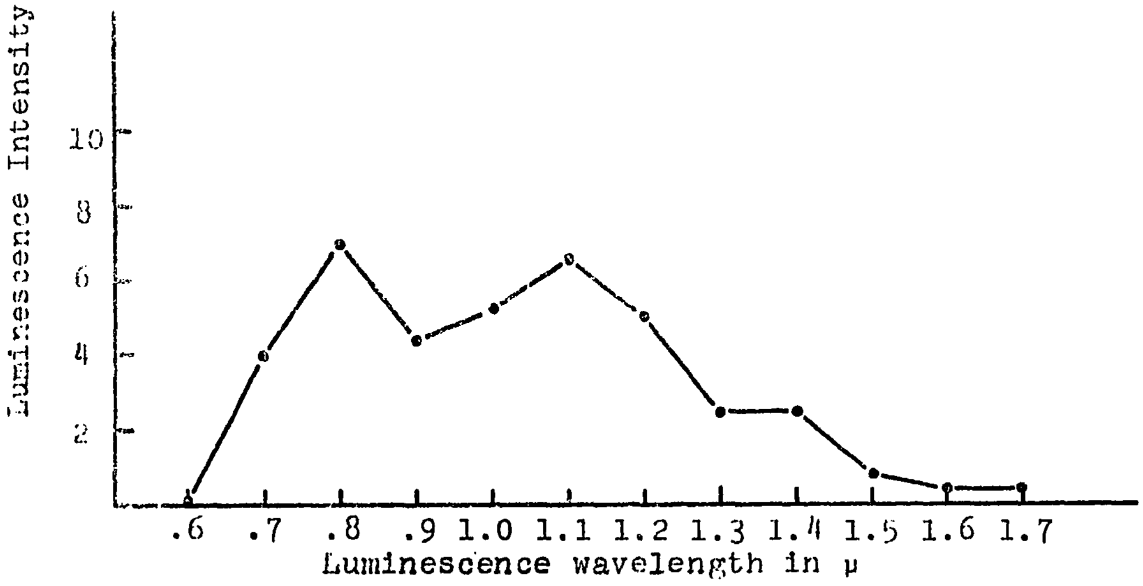

Figure 4-10. Luminescence spectrum of CdS:Cu.

the conductivity, provided that the electron mobility, $\mu_e$, remains constant. Bube, MacDonald and Blanc (37) have found that for CdS the Hall mobility varies only by a factor of two over the range of $n = 10^{10}$ to $10^{15} cm^{-3}$, and this is attributed to the change in electron mobility caused by the change in scattering cross section of recombination centers or trapping centers, as they go from charged to uncharged centers with the rise of the electron Fermi level. When the quenching radiation is introduced, the electron carrier density decreases markedly. Although the holes begin to contribute to $\sigma$, the net result is a quenching of the photoconductivity. This effect has been studied extensively. However, one may also expect a drastic decrease in the Hall mobility because of the possible cancellation of the electron and hole contributions. In fact, a

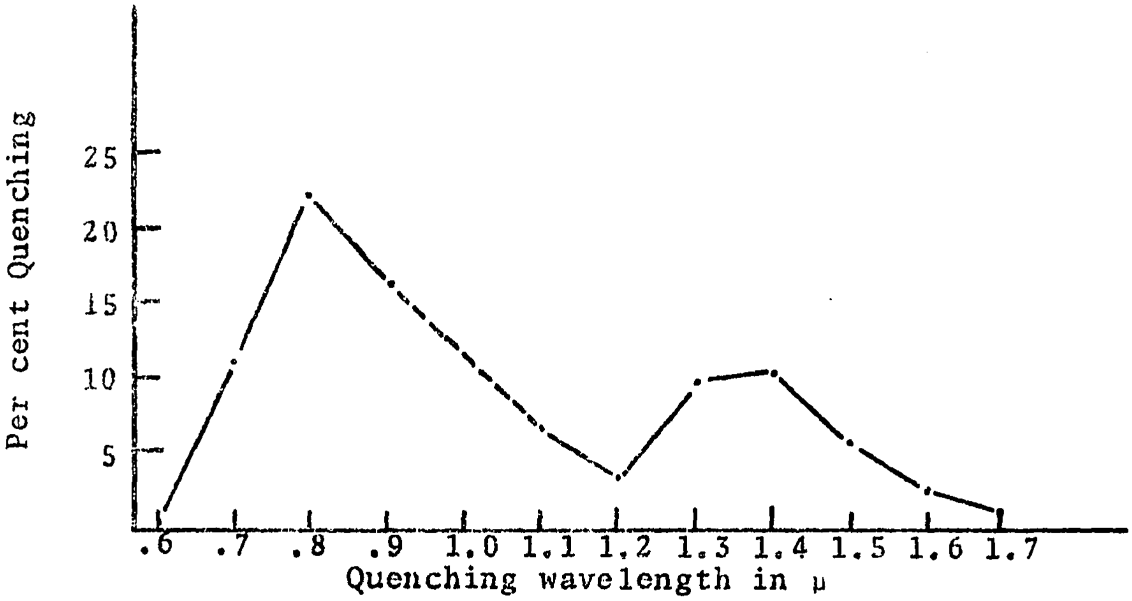

Figure 4-11. Quenching of 1.0μ luminescence in CdS:Cu.

substantial reduction of the photo-Hall mobility was observed previously but no spectral dependence of the quenching was reported.

We have measured the Hall mobility and its variation under infrared radiation in our samples. With band gap radiation only, the Hall mobility of the CdS crystals remains essentially constant (approximately $98\text{cm}^2/\text{V-sec.}$) over the range of electron density of $3 \times 10^9/\text{cm}^3$ to $3 \times 10^{11}/\text{cm}^3$, (Figure 4-12). The low mobility, compared to about $200\text{cm}^2/\text{V-sec.}$ in pure samples, is attributed to the Cu impurity. With the secondary infrared radiation, the change of the Hall mobility with respect to the frequency of the quenching radiation is shown in Figure 4-13. For comparison, the conductivity data are also included in this graph. Figure 4-14 shows the relation between $\sigma$ and $\mu_H$ under band gap radiation alone and under the combination of band gap and infrared radiation. The upper curve is produced by increasing the primary photoexcitation from point A to point B; and the lower curve by maintaining the constant point B primary excitation with increasing quenching radiation in the $0.8\mu$ to $0.9\mu$ range, causing a decrease in $\sigma$ and $\mu_H$ to point C. (The slight decrease of $\mu_H$ at higher $\sigma$ may be ascribed to the fact that for larger current through the crystal, the contacts become less ohmic, and the voltage drop across the contact increases non-linearly. Thus the measured electric field is somewhat higher than the actual value, causing the apparent drop of the Hall voltage.) With the infrared quenching, the mobility is seen to fall by a factor of

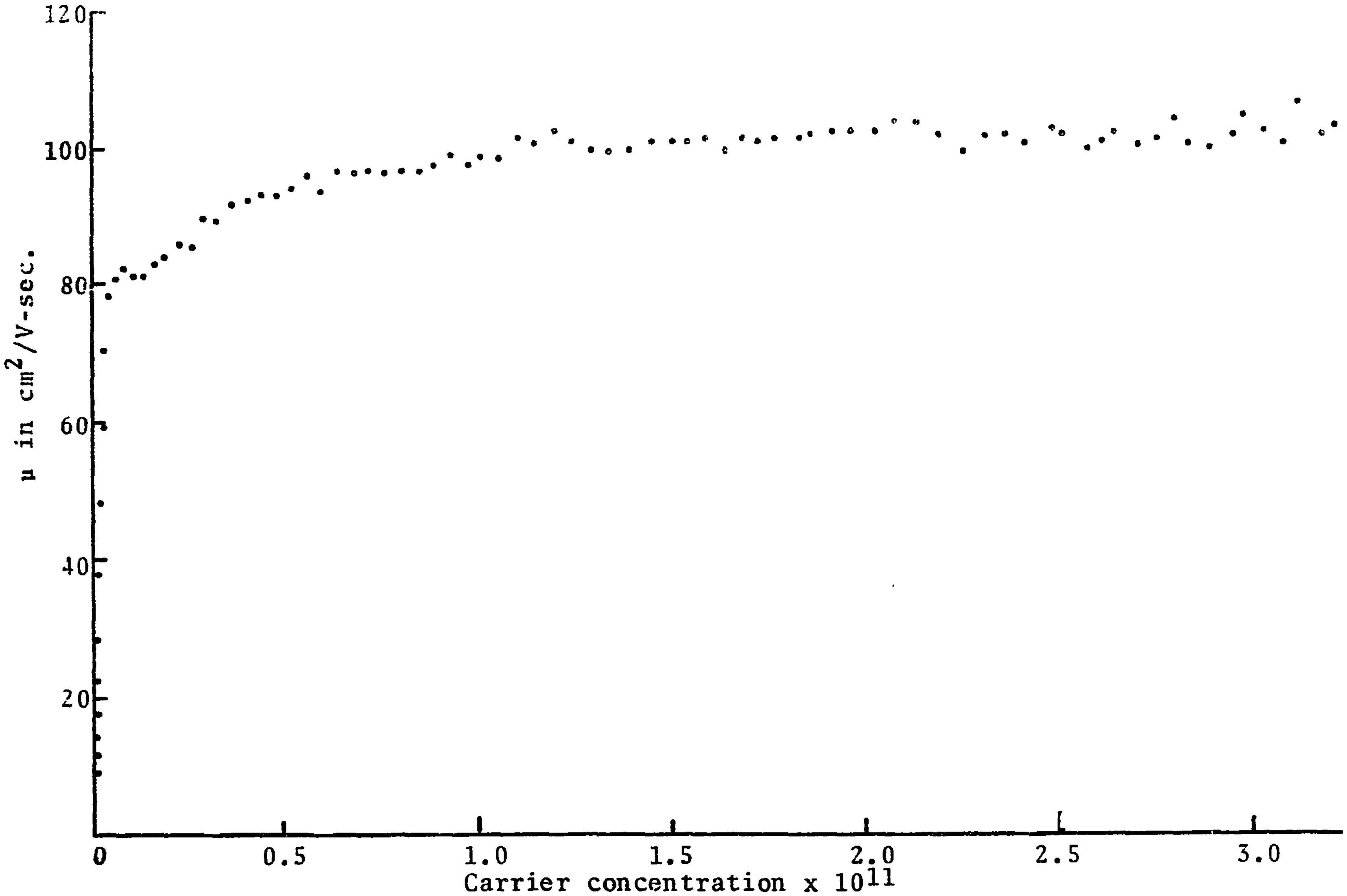

Figure 4-12. Hall mobility vs. intensity for CdS:Cu.

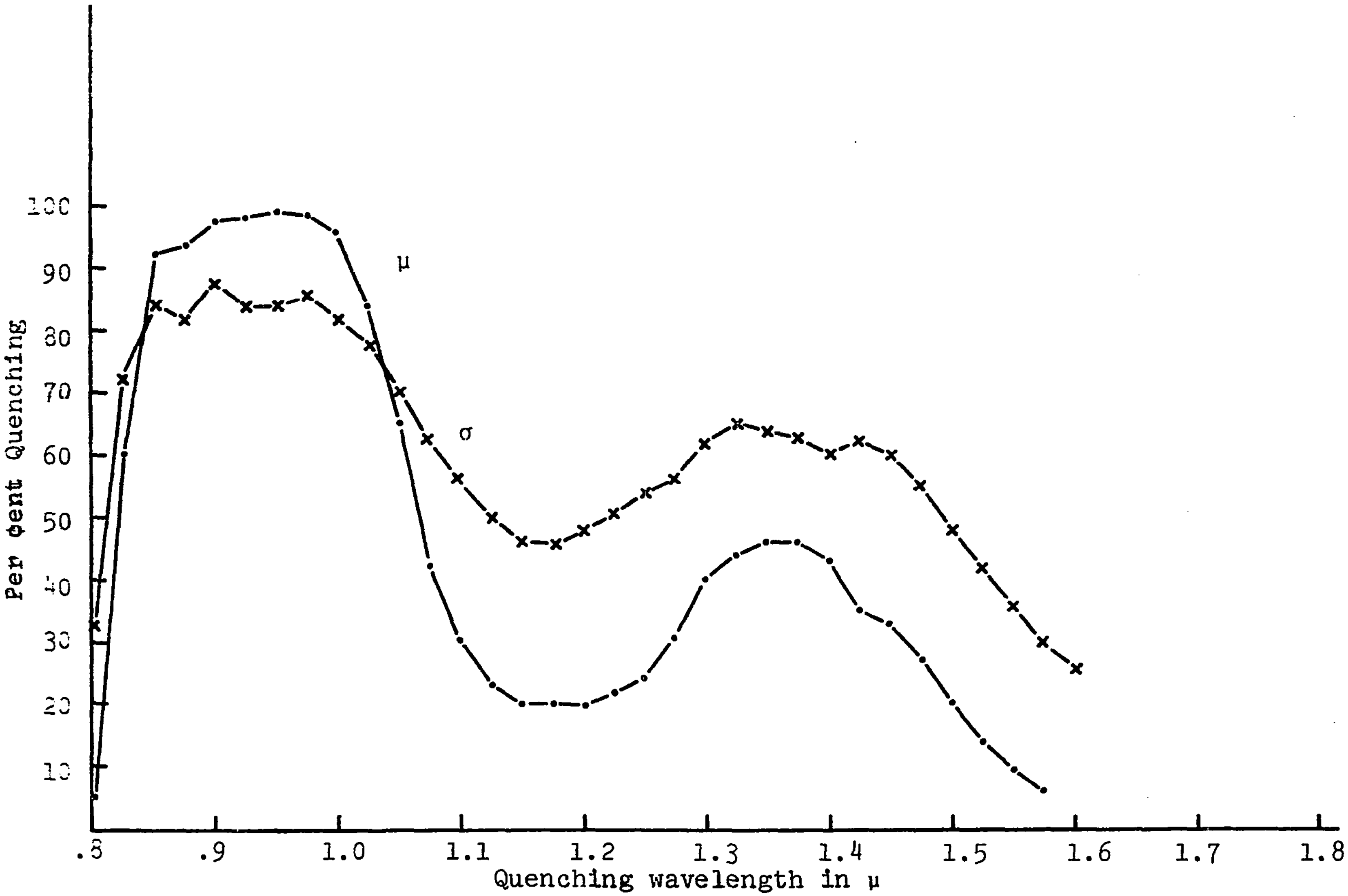

Figure 4-13. Photoconductivity and Hall mobility quenching in CdS:Cu.

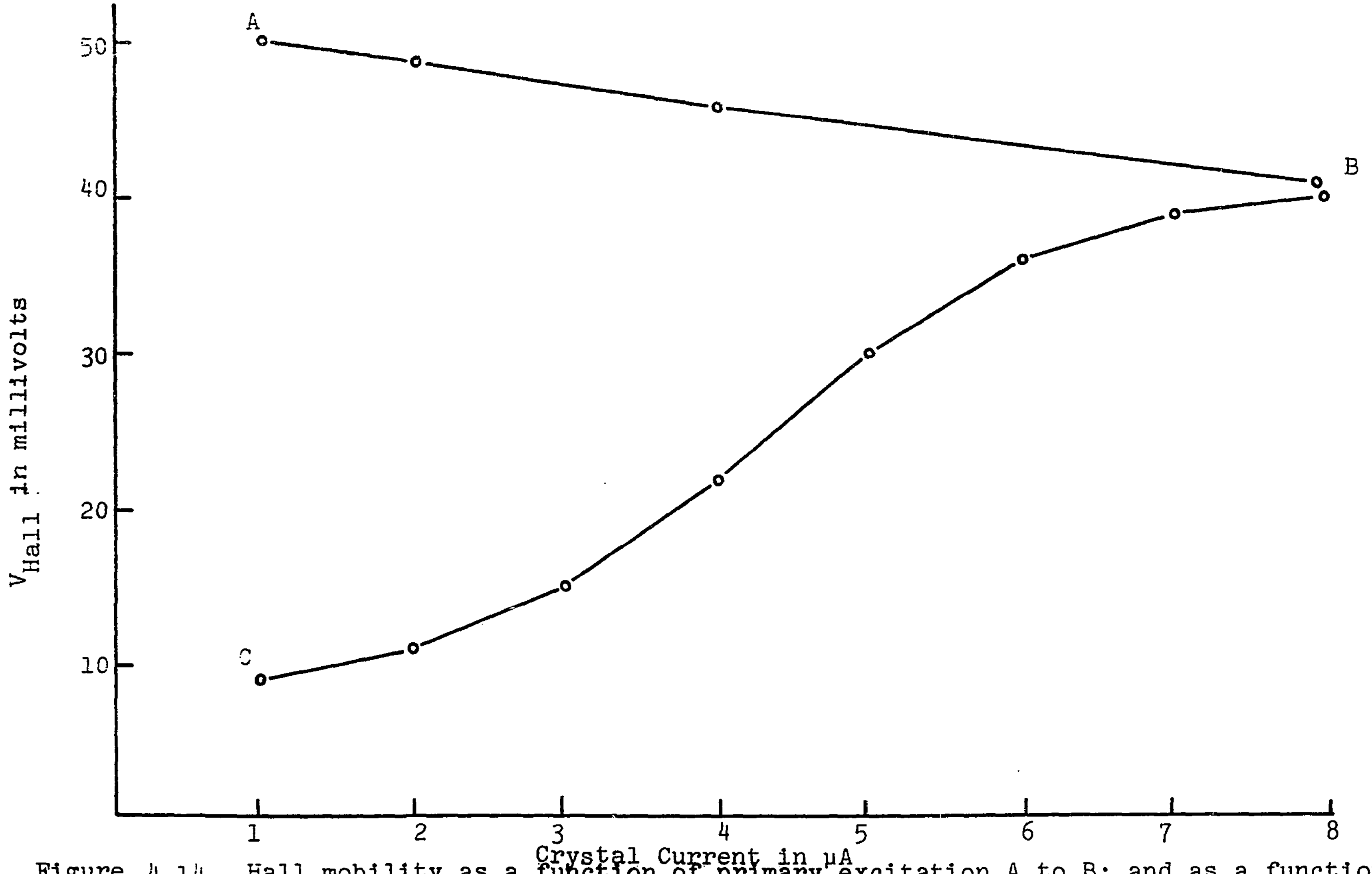

Figure 4-14. Hall mobility as a function of primary excitation A to B; and as a function of quenching intensity B to C, in CdS:Cu.

100, which is too large to be explained by the change of electron mobility due to charge scattering effects and is therefore attributed to the introduction of two carrier conductivity. The two maxima of quenching of the photo-Hall effect in Figure 4-13 occur at about the same wavelength as for the quenching of the 1.02μ luminescence. Similar experiments on the quenching of the Hall mobility have been performed for the ZnS samples. The results are given in Figures 4-15 and 4-16. Due to contact difficulty and low signal, the results are marginal, however they show the two peaks at 0.9μ and 1.25μ, similar to those found in the luminescence experiments.

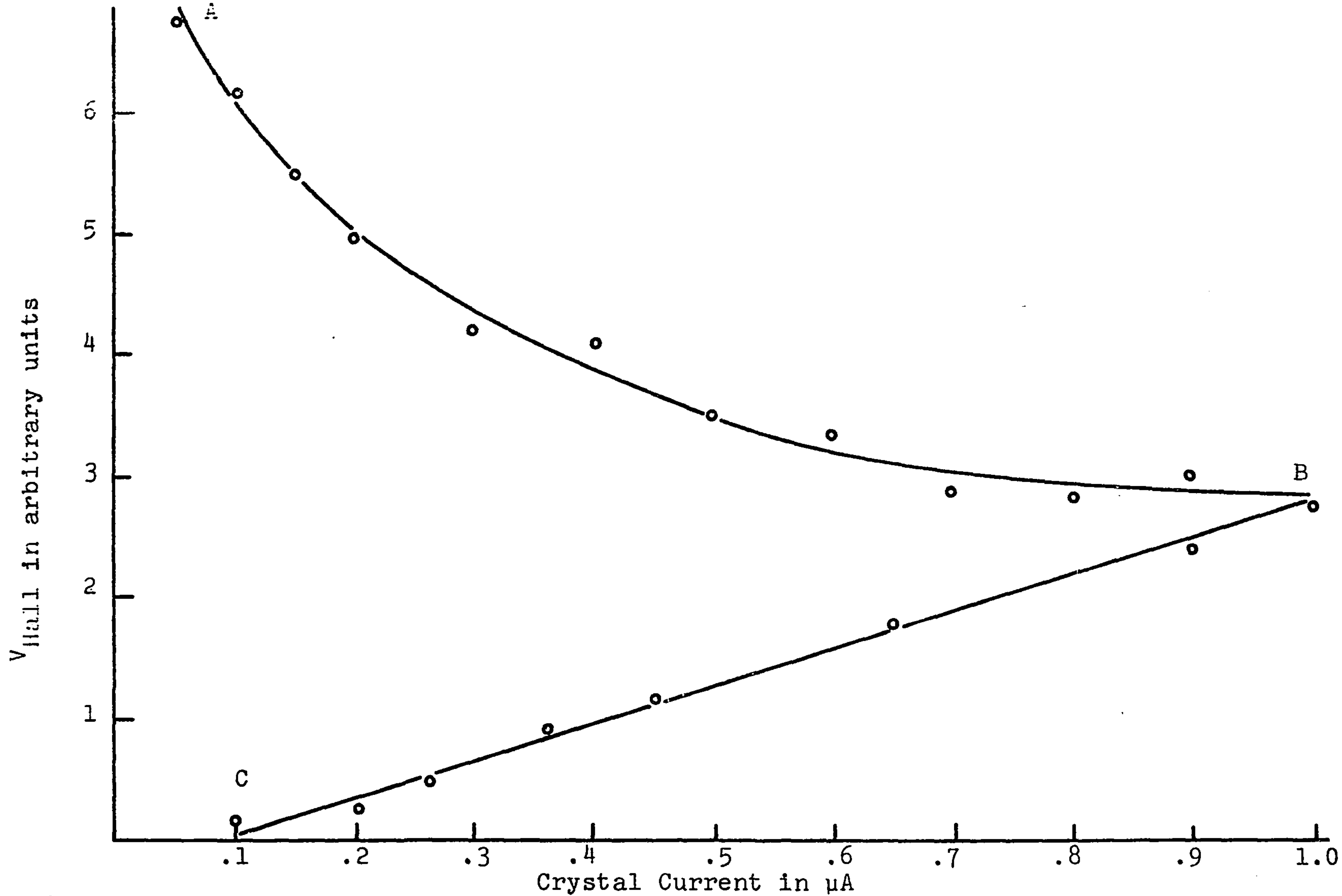

Figure 4-15. Hall mobility as a function of primary excitation A to B, and as a function of quenching intensity B to C, in ZnS:Cu.

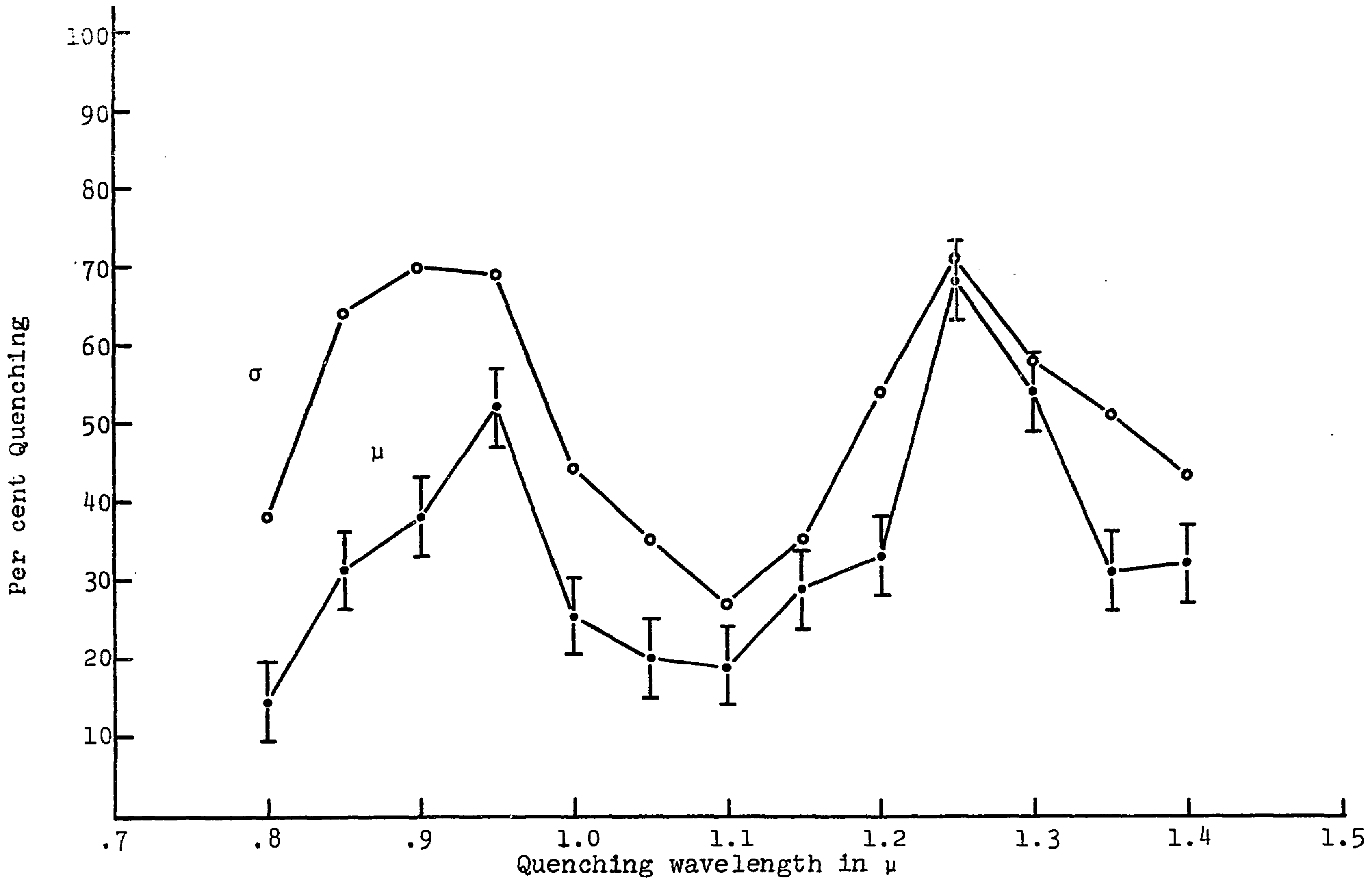

Figure 4-16. Photoconductivity and Hall mobility quenching in ZnS:Cu.

# CHAPTER V

# APPARATUS

## I. Luminescence Apparatus

The luminescence equipment was designed to perform the following experiments: 1. Measure the luminescence of single crystal samples from 0.4μ to 3.5μ, using electron excitation. 2. Examine the effects of secondary radiation on the luminescence. 3. Although not a point of primary emphasis, one can derive some information on the transient luminescence response.

Of the several possible modes of operation which could be used to satisfy these requirements, the following combination of methods were selected.

### Electron Beam Excitation

Electron beam excitation of luminescence offers several advantages over optical excitation, and, since the nature of the luminescence is relatively independent of the mode of excitation, it was selected over optical excitation. The same experiments are available using electron beam excitation, as for optical excitation, except the optical excitation spectrum cannot be done. The advantages of electron excitation are: (a) Optical isolation is not necessary. In general, either optical filters, monochromators, or mechanical means are necessary to prevent the excitation radiation from reaching the detector. This may be a great advantage if the optical excitation wavelength is near the wavelength of luminescence. (b.) Modulation is produced electronically by chopping the electron beam, obviating the need for mechanical modulation. The luminescence itself is modulated by the beam, and the modulation frequency can be selected for optimum detector response, without regard to mechanical limitations. (c.) The reference signal is taken directly from the same modulation source. (d.) Greater luminescence intensity can generally be reduced than with optical excitation, which is useful in searching for possible luminescence. However, quenching experiments are ordinarily done at very low luminescence levels for maximum sensitivity.

To produce stable luminescence intensity the vacuum system must be capable of producing vacuum on the order of $10^{-6}$Torr. Also, the electron beam controls and power supplies must be stable and drift free.

## A.C. or Modulated Luminescence

Although for visible luminescence it is possible to monitor the D.C. or steady state signal using photomultiplier detection, it is not practical for i.r. luminescence. Infrared detectors are generally operated at a signal frequency which will produce maximum detectivity, and in the case of PbS detectors, is about 200 Hz.

## Unmodulated Secondary Radiation

Steady, unmodulated secondary radiation is used, so that there will be a minimum of interference with the luminescence detection. Since the intensity of the secondary radiation scattered into the detection system may be large compared to the luminescence, it is necessary that it have no intensity modulation, such as a 60 Hz ripple.

## Block Diagram

A block diagram of the luminescence equipment is shown in Figure 5-1. The overall operation is described below. A detailed description of individual components follows in the next sections.

The crystal sample is mounted at the intersection of the excitation, secondary radiation, and detection arms of the gun assembly. It is mounted on a metal dewar feedthrough at the common foci of the secondary radiation collimation mirror, electron beam, and detector assembly. The detector arm and secondary radiation arm are perpendicular to each other, but have been drawn in the same plane for clarity. The dewar allows for cooling of the sample to 77°K.

Electron beam excitation is produced by the modified cathode ray tube electron gun G, the beam current to the crystal being modulated by the modulation and reference oscillator. The beam current, position, and beam focus are controlled by the electron gun control, a modified oscilloscope. A 10 KV power supply produces the final electron acceleration. The

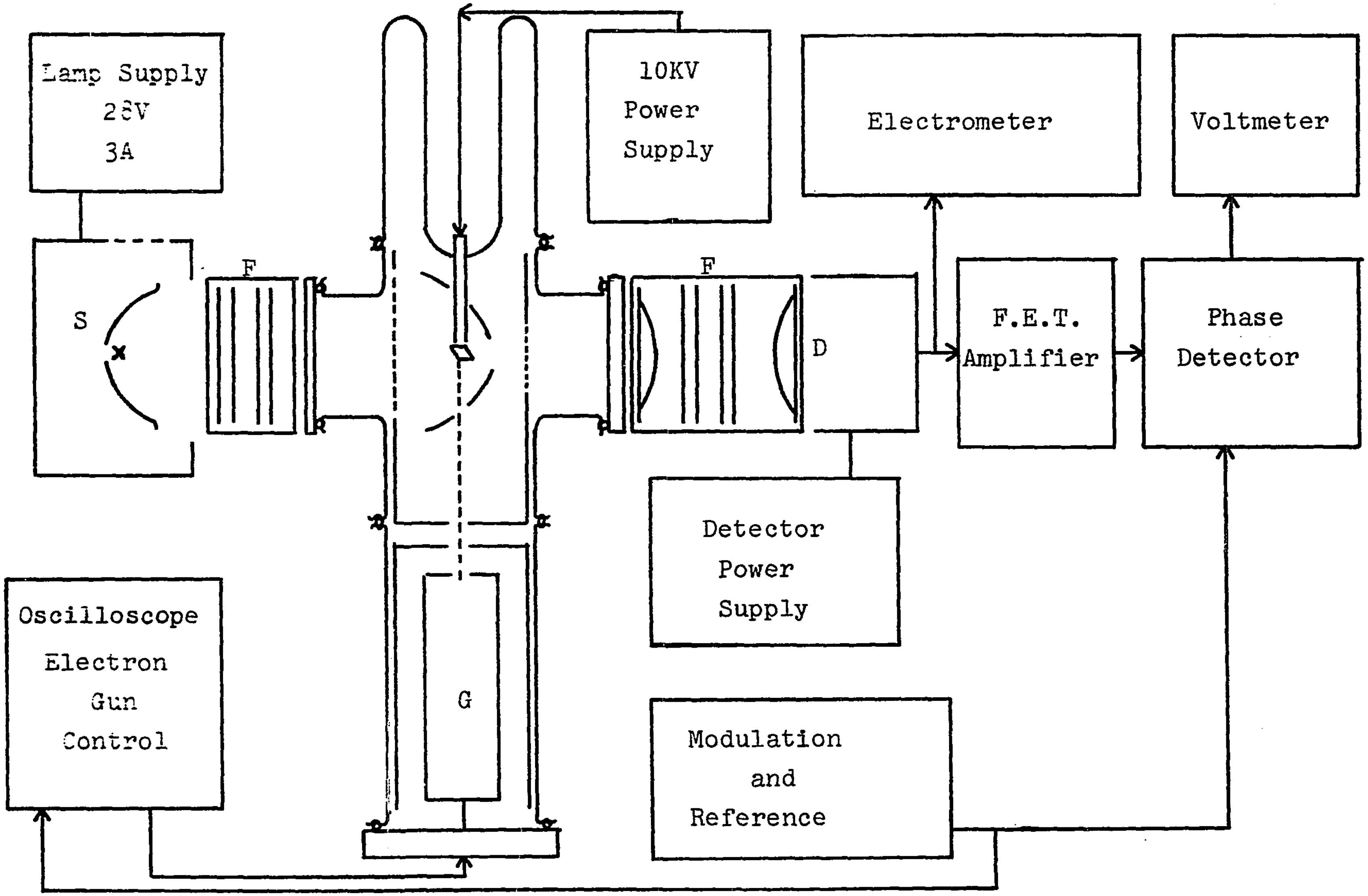

Figure 5-1. Block diagram of the luminescence apparatus: S, quenching source; G, electron gun; F, filters; D, detector.

luminescence radiation is focused through appropriate filters F, onto the detector, producing an A.C. signal, which is amplified by the field effect (f.e.t.) transistor amplifier, synchronously phase detected, and the integrated D.C. voltage is monitored by a voltmeter. For photomultiplier detection, an electrometer is used to monitor the photomultiplier current. Secondary radiation from the source S, is focused onto the crystal using short focal length mirrors. The light gathering power of this system is high, allowing near optimum utilization of the light source and filters. The light is monochromated by thin film dielectric filters F. A low ripple D.C. power supply is used to power the lamp. This is essential since scattered light from the sample may reach the detector, and must contain no A.C. component. An oscilloscope is used to monitor the rectified A.C. signal from the phase detector.

## Optical Assembly

In this and following sections are discussions of the individual components which comprise the luminescence system. Detailed descriptions and design philosophies are given.

*Quenching optics.* The secondary radiation, or quenching source, which was adopted is a 75 W tungsten-halogen quartz lamp, Figure 5-2. Several factors influenced its selection over other available lamps such as the various arc lamps. Compared to arc lamps, which have a spiked line spectrum superimposed over a broad blackbody spectrum, the tungsten lamp has the normal smooth blackbody type of spectral output. This

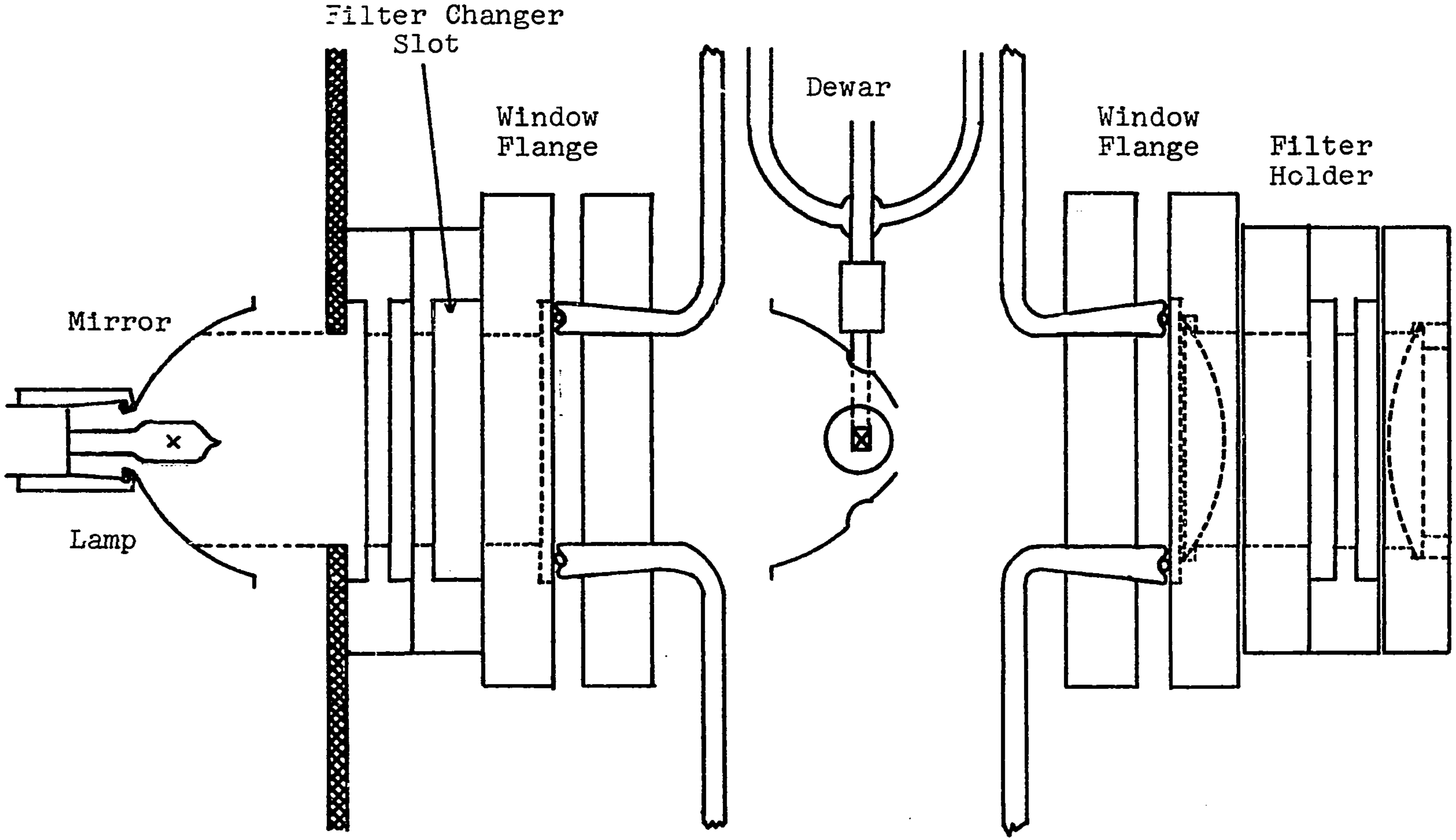

Figure 5-2. View of the quenching optics, left; crystal and condenser mirror, center; and detector optics, right.

is necessary for convenient analysis of spectral response of quenching or excitation due to the secondary radiation. The lamp operates at a color temperature of 3000°K, three hundred degrees higher than ordinary tungsten bulbs, with a brightness of 1600 lumens. Usable radiation is available from the near U.V. out to the i.r. cutoff of the quartz envelope, 3.5μ. Brightness is not as high as arc lamps but its small size permits the use of very short focal length optical design. This allows the focusing of up to 80 per cent of the lamp output into a nearly parallel beam 2 inches in diameter, necessary for the efficient use of the 2 inch square dielectric filters. No other lamp commonly available allows such a configuration. The mirror focal length is 3/8 inch, giving an effective f-number of about f/0.25. Due to the high bulb temperature, a metal reflector must be used. The quartz bulb, in addition to the extended i.r. transmission requires no cooling except air convection. (The bulb envelope operates near 600°C for the halogen cycle to be effective.) Bulb life is rated nominally at 2000 hours. Bulbs with higher operating temperature (3400°K color temperature) are available with reduced lifetime.

The optical assemblies used in both the luminescence and photoconductivity experiments are constructed from standardized assembly blocks. The aluminum blocks are 2 x 3 x 1/2 inch with a 1-1/2 inch hole as shown in Figure 5-3. Four 0.250 inch holes receive metal rods for assembly. The individual blocks are modified to hold lenses, filters, detectors or other components such as the filter changer, and are attached to the

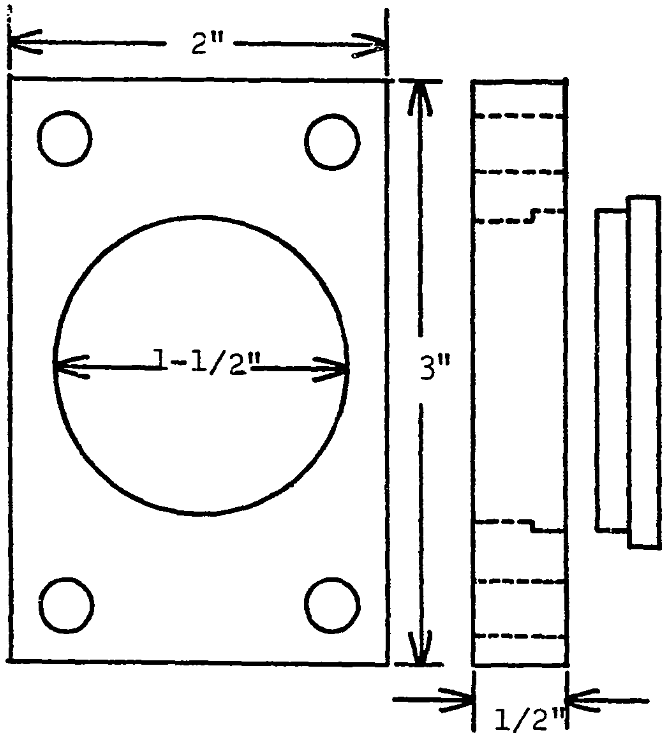

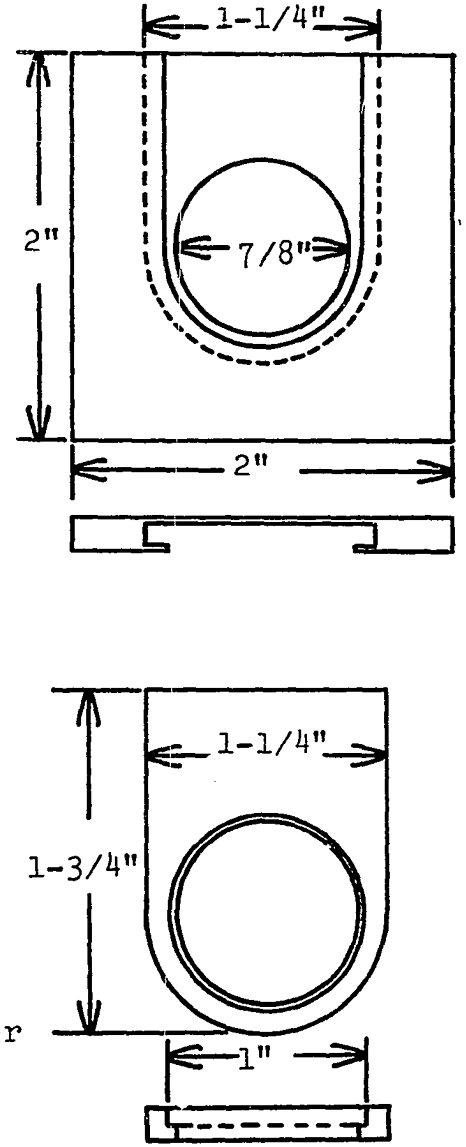

Figure 5-3. Optical blocks, left; 1 inch diameter filter adapter for filter changer, right.

equipment with the 1/4 inch steel pins. The quenching light source, window flanges and photomultiplier housing have matching holes for attachment. This construction allows for a great variety of optical arrangements and quick assembly.

The parallel light from the tungsten-halogen lamp is monochromated with thin film dielectric filters (to be discussed in the next section) held in the filter changer, Figure 5-4. The filter changer slides in the 2 x 3 inch optical blocks. The blocks are arranged so that air cooling of the filters can be used, but still keep out extraneous light. The monochromated parallel beam is focused onto the crystal by the condensing mirror inside the vacuum chamber. It is identical to the lamp mirror except for four holes (Figure 5-2) for the dewar extension, electron beam, detector radiation and a blank space opposite the detector hole to keep quenching radiation from being directly reflected into the detector.

Dielectric interference filters. The filters used for monochromating the quenching radiation and for selection of luminescence bands in the detector assembly are commercial thin film dielectric filters. They have a typical transmission of 35 per cent at their peak and a 3 per cent bandwidth; i.e., a 1μ filter will have a 0.3μ bandwidth. They are blocked at all other wavelengths by absorbing layers. They require forced air cooling to avoid destructive heating by the light source. The absorptive side of the filter must be faced away from the lamp.

A comparison of the light gathering power of the lamp,

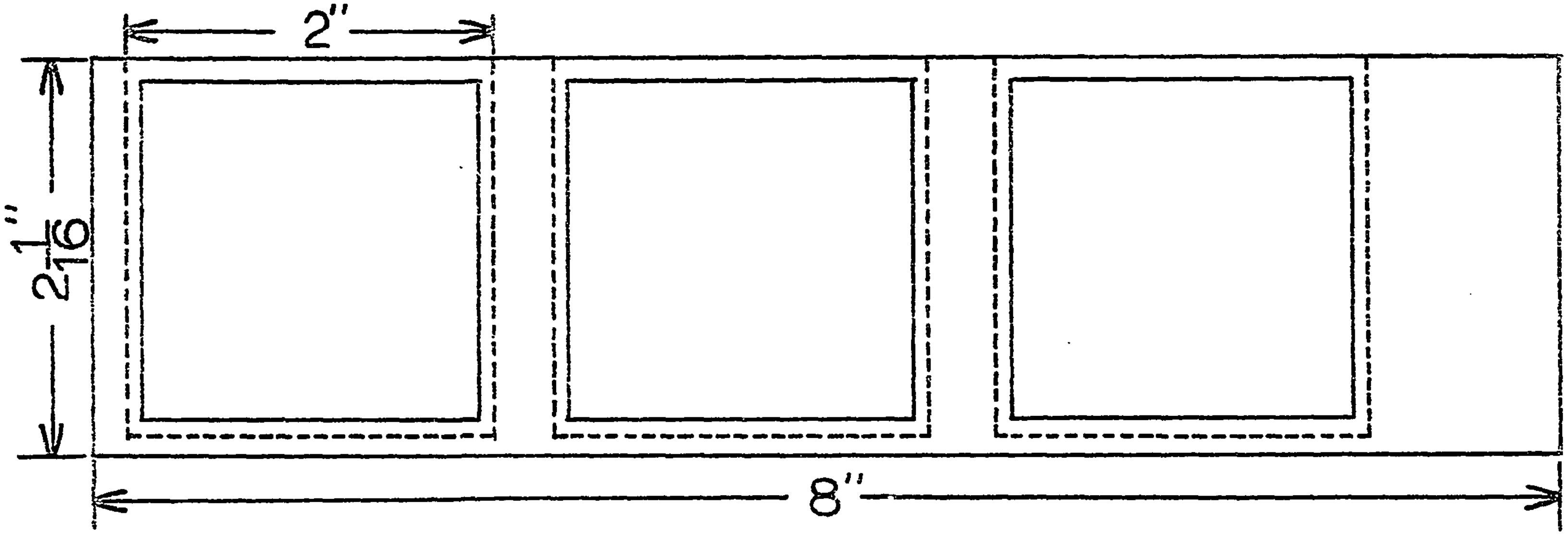

Figure 5-4. Filter changer.

filter, and reflector combination, compared to an f/4 monochromator shows that the filter assembly is capable of focusing about 60 times as much light on the sample. This is strictly a geometric comparison, assuming 30 per cent transmission for the filters and 100 per cent transmission for the monochromator, and equal bandwidths. Poor focus, and mirror holes reduce this factor to some extent. Thus, for the high intensity required for luminescence quenching, the filter assembly is used.

Normalization filters. In order to produce constant intensity quenching radiation as a function of frequency for the thin film filter assembly, neutral density normalizing filters were prepared. They cover the range of 0.8μ to 2.7μ. By virtue of the method used, the normalization is valid only for the tungsten-iodine bulb operating at its rated power, and the specific filter used in the preparation. Filters replaced by breakage generally will have some variation in bandpass and peak transmission, and may not match the neutral density filter. It was found to be very difficult to produce normalization closer than about 10 to 20 per cent error from one filter to another.

Preparation of normalization filters. The production assembly is shown schematically in Figure 5-5. The light source and filter holders are those used in the luminescence experiment, so the normalization is specifically for that assembly. The source with the filter to be normalized illuminates the detector through the clear glass plate in the vacuum system,

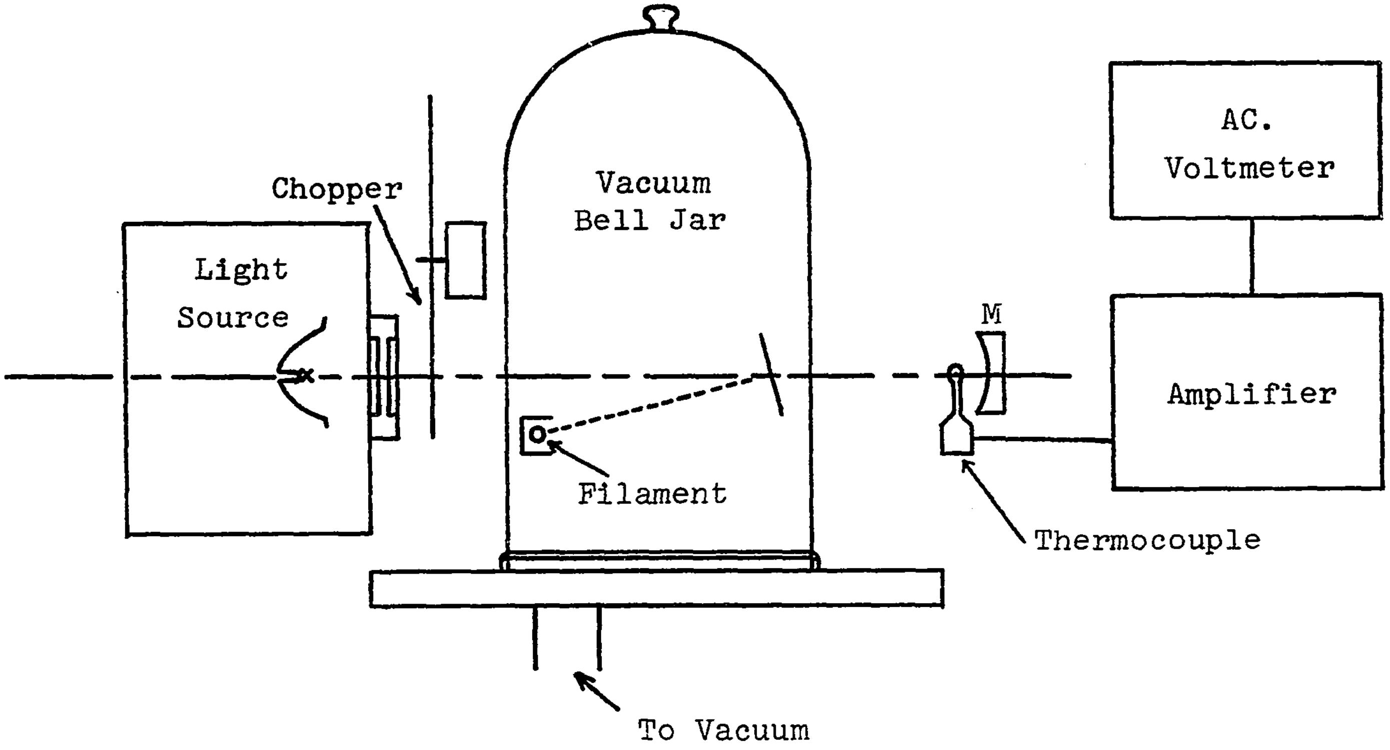

Figure 5-5. The neutral density filter apparatus.

and metal evaporation is continued until the detector signal falls to a predetermined level matching the power transmitted by the weakest filter in the set. The filter faces the filament and is slightly canted with respect to the optical beam. This causes no error in the normalization except that multiple reflections are prevented, whereas in the experimental set-up, multiple reflections do occur. In some cases it was necessary to select the proper density by trial and error to get the proper intensity in the final experimental set-up. Finally, each combination was tested in its experimental configuration. By careful selection, normalization of each filter was held to within about 5 per cent of the intensity of the weakest filter.

Evaporation. The neutral density filters were made from gold evaporated in vacuum onto lantern slide glass. Gold was chosen over aluminum since aluminum films changed optical density by 20 to 30 per cent immediately upon contact with air. Note that the method of monitoring takes into account the transmission of the glass at the wavelength used. The filters must be forced air cooled to prevent cracking when used with the lamp, or be placed on the back side of the interference filters, away from the lamp.

Detector optics. Light from the sample is focused onto the detector by the detector lens-filter assembly shown in Figure 5-2. The quartz lenses and quartz vacuum window are usable to the i.r. cut-off of quartz, near 3.5$\mu$. The assembly uses one interchangeable optical blocks and can be adapted to hold thin film filters, liquid filters, or the 1/4 meter monochromator can be inserted in the optical line. For visible luminescence a 1P21 photomultiplier was used. Its housing, shown in Figure 5-6, mounts onto the optical block pins. For infrared detection a PbS detector which is mounted on one of the optical blocks is used. The spectral response of the PbS detector is from about 1μ to 3.5μ.

## Electron Gun

The electron gun is mounted on an aluminum flange, Figure 5-7. It is a standard electrostatically focused and deflected gun taken from a cathode ray tube. The normal oxide coated cathode has been removed and a directly heated tungsten coil serves as the cathode. It can deliver up to 50 ma. at about 1.0 KV. The beam receives a final acceleration of 10 KV before reaching the crystal. The gun is tilted off axis to minimize light from the cathode from reaching the sample. This prevents excessive dark current when the photomultiplier detector is used. The grounded can around the upper part of the gun and the post acceleration can around the sample assembly provide a uniform accelerating field between them. The hole in each can is fitted with wire gauze to prevent field distortion and defocusing of the beam. The upper, or post acceleration can is connected to the high voltage lead of the dewar, and provides a field free space inside.

The electron gun supply voltages are taken from an ordinary oscilloscope. The filament supply, however, is separate

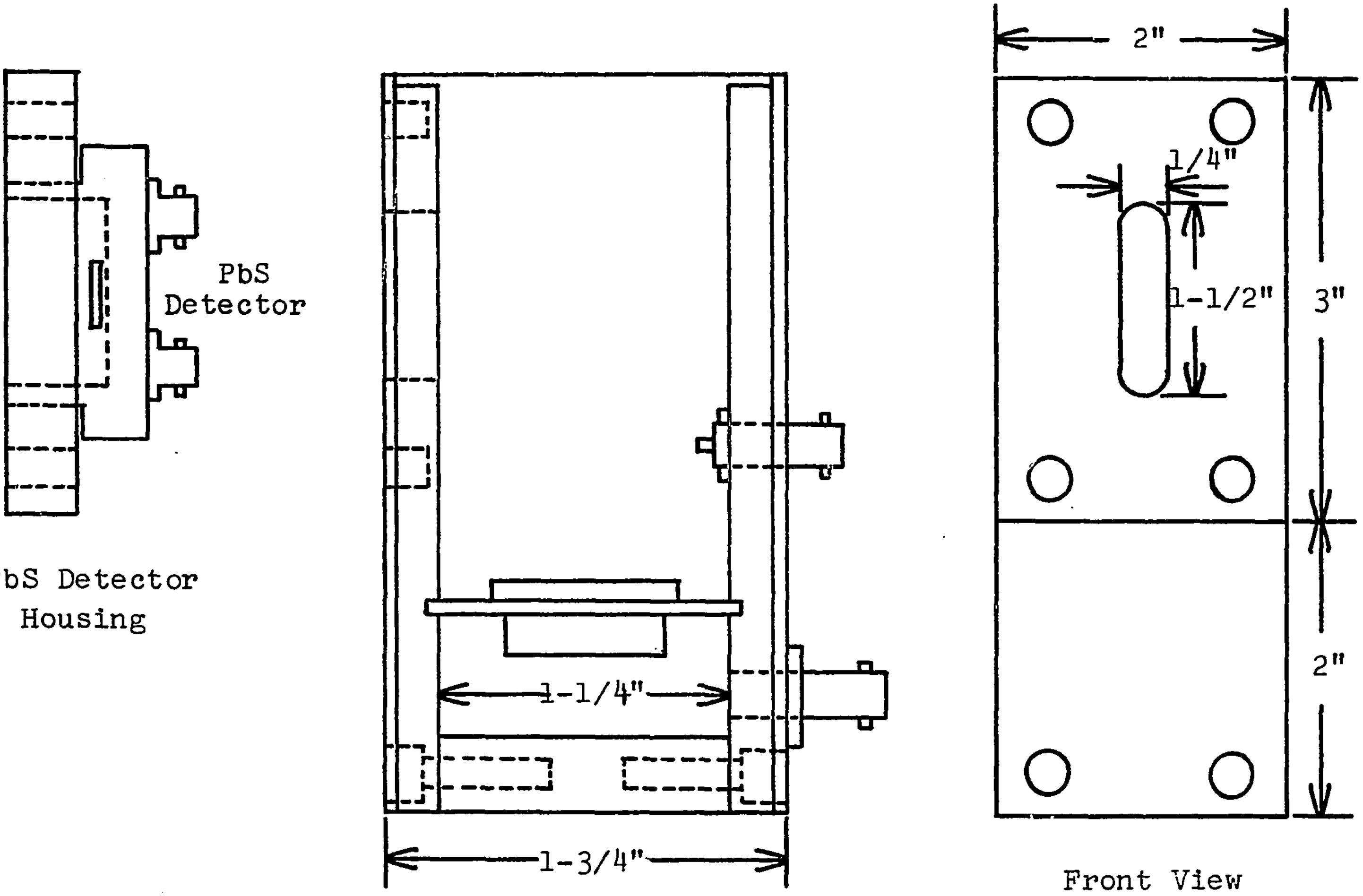

PbS Detector Housing

Side View

Front View

Photomultiplier Housing

Figure 5-6. Detector housing; PbS, left; photomultiplier, center and right.

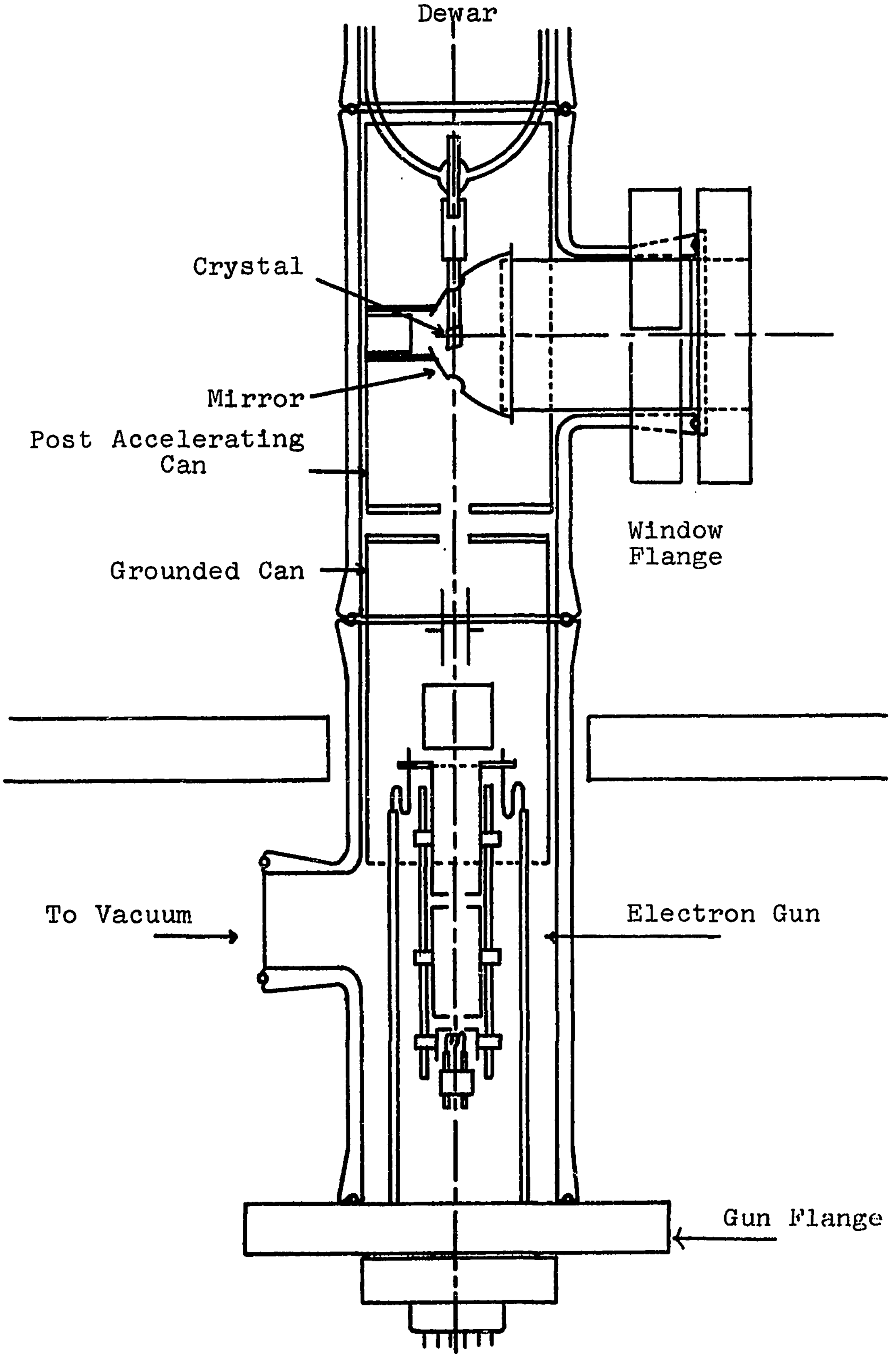

Figure 5-7. Luminescence gun and crystal mount assembly.

to allow for the variation in cathodes used, and the heater voltage is variable from zero to 12 V, and up to 20 A. The heater supply is isolated for 2000 V by the transformer, Figure 5-8. The gun controls; intensity, focus, and x, and y positions are operated from the front of the gun control oscilloscope. The square wave beam modulation on the x axis moves the beam on and off the crystal producing luminescence modulation.

## Luminescence Vacuum System

The luminescence vacuum assembly is constructed of three sections of 2 inch Pyrex brand pipeline with "O-ring" flanges. The lower section holds the electron gun, which is mounted through the bottom opening on an aluminum flange. The lower section also connects to the pumping system through a 1 inch side arm. The middle section is open at both ends and has two 1-1/2 inch arms perpendicular to each other for the optical window flanges. The upper section is a nitrogen dewar with a tungsten rod feed-through on the bottom. The parts assemble with standard O-rings and Pyrex flange connectors. Special window mounting flanges were constructed which have mating holes for the optical building block dowell pins. The gun flange bolts to the pipeline with a 2 inch clamp, and has an O-ring sealed feed-through, made from a cut-off 9-pin miniature vacuum tube, for gun connections. The middle section is painted black and shielded with black metal cylinders outside the glass.

C.R.T. Connector
Pin:
1. Cathode, High Voltage
2. N.C.*
3. X
4. Focus
5. N.C.
6. Y
7. Ground
8. X
9. Y
10. Control
11. N.C.

Luminescence Gun
Feedthrough Connector
Pin:
1. Ground
2. Filament
3. Filament
4. X
5. Control
6. Y
7. X
8. Focus
9. Y

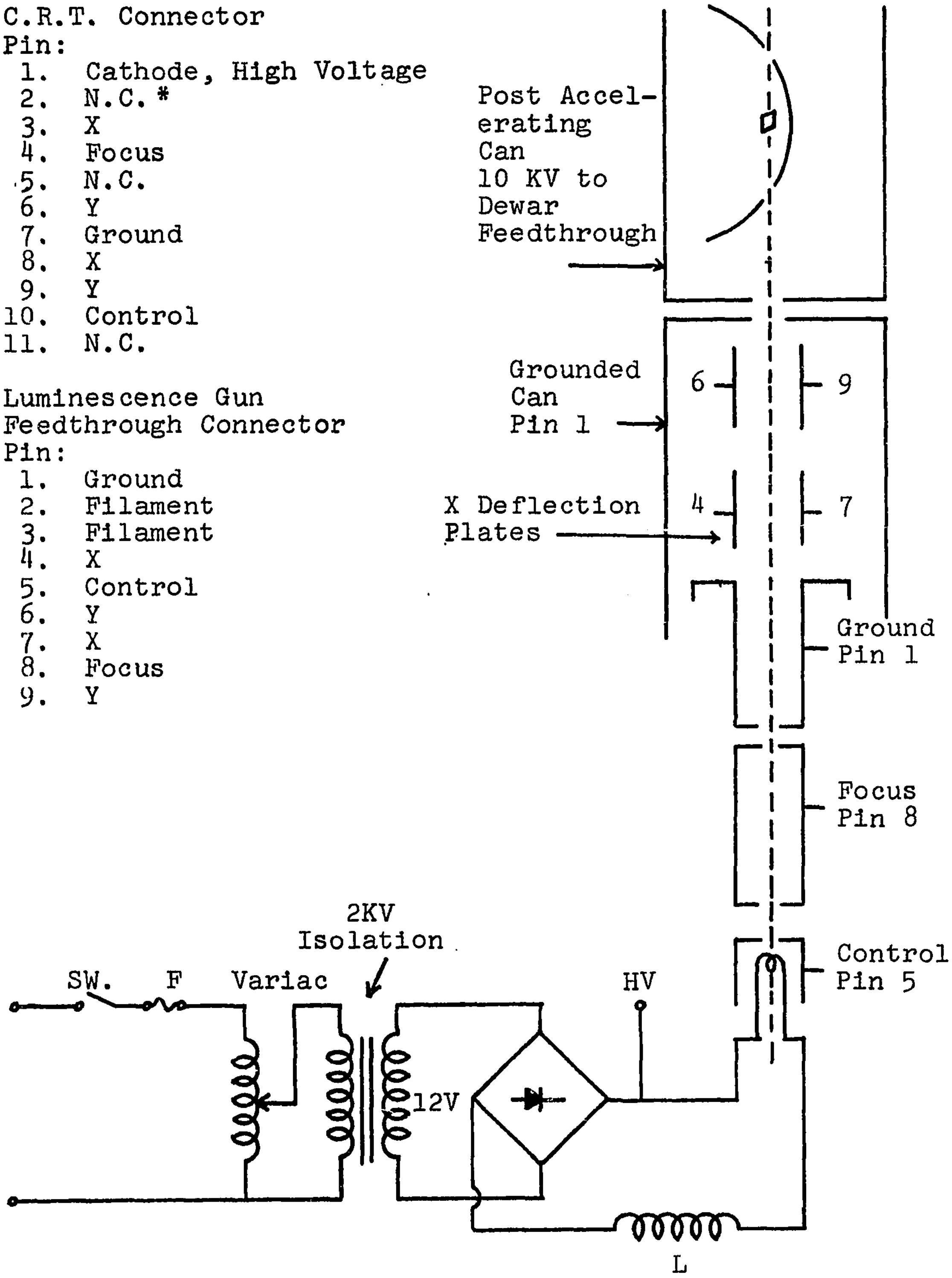

*N.C. (not connected)

Figure 5-8. Electron gun filament circuit and pin connections.

The grounded can is held in place by an aluminum washer held in the O-ring flange groove, and the post-acceleration can is held by the two metal sleeves in the window arms. The post-accelerating can, sleeves, and back of mirror are blackened by a chemical blackening process to reduce scattered light.

The sample is mounted on an adjustable brass rod that clips onto the tungsten dewar feed-through, and is adjusted to position the sample at the focus of the mirror. There is an electrical connection from the feed-through to the post-acceleration can. The sample is mounted to the rod with conducting silver paint.

## Detection and Signal Processing

The detection and signal processing system consists of the detector assembly preamplifier, phase detector and D.C. voltmeter for monitoring the signal level.

Detector. Since a large solid angle about the sample is required by the quenching system, and little room remains for the detector optics, an f/1 imaging system focuses the luminescence radiation onto the detector, either a photomultiplier or PbS detector. For visible detection, the 1P21 photomultiplier is highly sensitive and allows very low levels of luminescence to be used. Also, the D.C. level of luminescence can be measured in addition to the modulated signal. In the case of infrared detection, the PbS detector used affords about the best sensitivity available in the 1μ to 4μ range. However, its sensitivity is about two orders of magnitude lower than that of a photomultiplier, and larger excitation and luminescence levels must be used. The characteristics of PbS detectors are such that maximim detectivity, or signal to noise ratio is achieved at a modulation frequency of about 200 Hz. The signal frequency of 200 Hz was selected for this reason.

Amplifier. A low noise, tuned, field effect transistor amplifier is used to amplify the detected signal, Figure 5-9. The design is a modified form of a published low noise amplifier (38), having an extra feedback loop. The feedback, coupled by a twin tee network, gives strong negative feedback except at the tuned frequency.

The 2N2500 field effect transistor has excellent low noise characteristics and minimizes system noise due to the critical first stage of amplification. The circuit has a gain of 60 db. and voltage output of 20 V peak to peak.

Phase detector. The amplified signal is synchronously rectified by the phase detector, which gives a D.C. voltage output proportional to the signal. The phase detector is of standard design, modeled after several which have been built in this laboratory in the past (39). The circuit is given here for reference, Figures 5-10, 5-11. There is no phase shift oscillator necessary here since the signal frequency is low. Thus, the signal goes directly to the amplifier, phase splitter and diode bridge. The reference voltage from the modulation oscillator drives the Schmitt trigger which supplies a square wave to the phase splitter, to gate the diode bridge

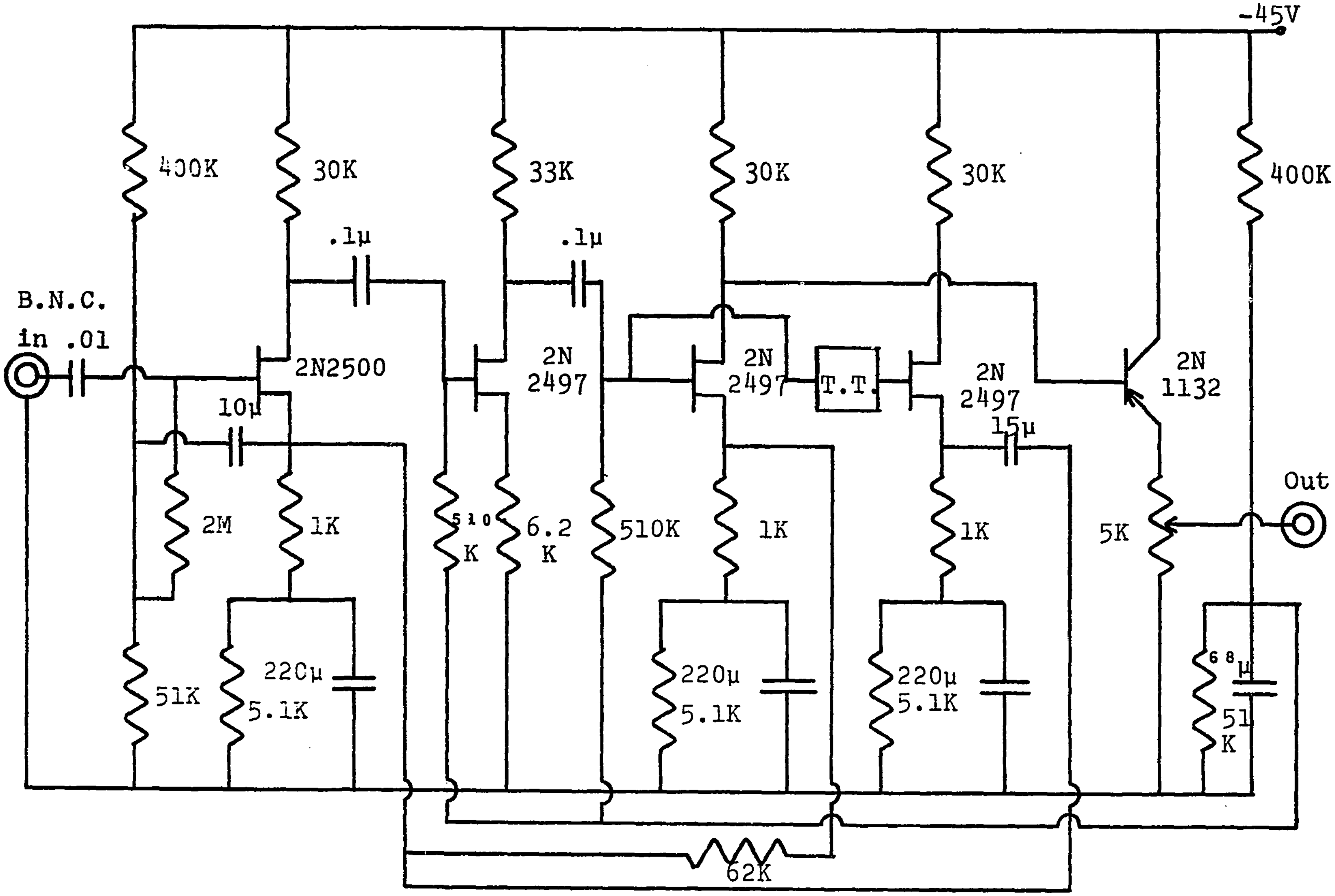

Figure 5-9. Low noise f.e.t. preamplifier.

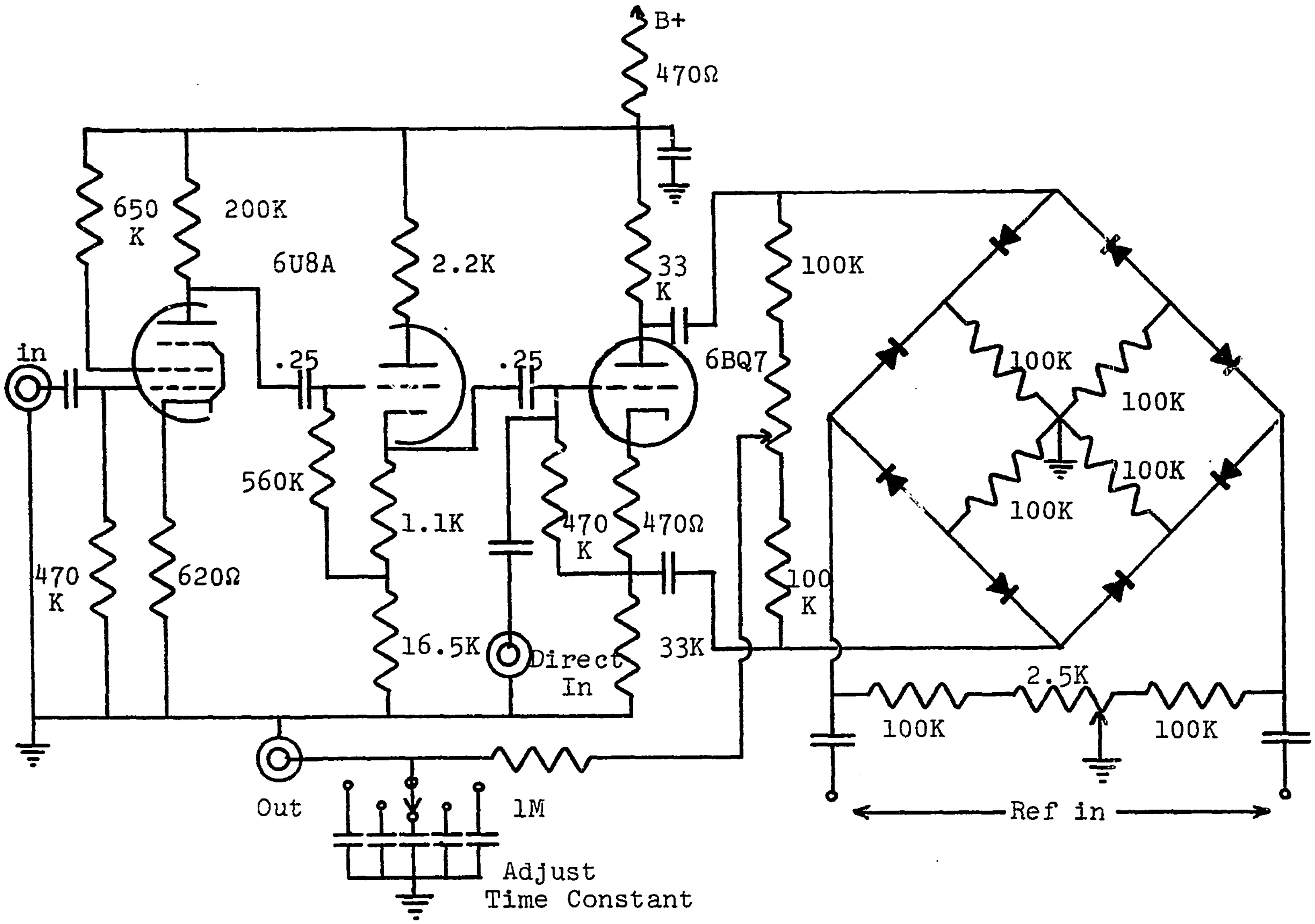

Figure 5-10. Phase detector, signal section and diode bridge.

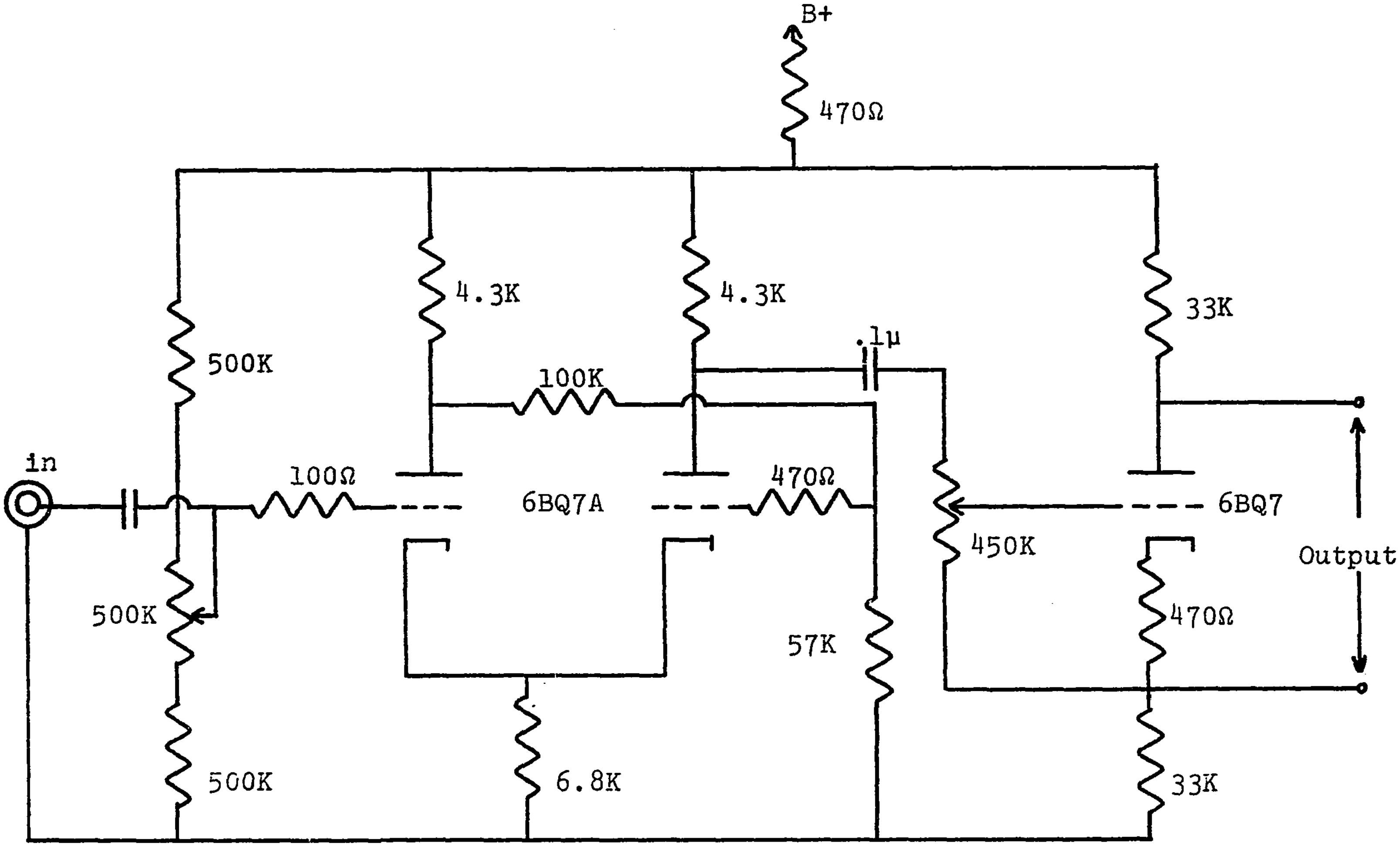

Figure 5-11. Phase detector, reference section.

in synchronization with the signal. The reference voltage to the bridge is a 30 V square wave, and allows the bridge to handle signals up to 30 V. The linearity of the bridge has been examined and is quite good.

The bridge output signal is capacitively integrated, with an RC time constant of several seconds. The integrated signal is monitored with a commercial vacuum tube voltmeter. It is necessary to use a vacuum tube voltmeter since the output impedance of the phase detector is about 1 megohm. An oscilloscope monitors the output of the phase detector for a visual display of the rectified signal.

The high voltage post accelerating supply is shown in Figure 5-12, and is of standard design. The low ripple lamp supply is shown in Figure 5-13. Very large capacitors and chokes are used to minimize 60 Hz ripple.

## II. Photoconductivity and Hall Mobility Apparatus

The photoconductivity and Hall mobility apparatus was constructed to measure photo-Hall mobility quenching effects in high resistivity samples. Crystals with resistance as high as $10^9 \Omega$ were examined. Photoconductivity and Hall mobility were measured as a function of some optical variable such as intensity of primary radiation, wavelength, or intensity of secondary radiation, with fixed primary excitation. Photo currents as low as $10^{-9}$A and Hall voltages of 1 mV were measured.

The system operates in an A.C. mode; the Hall voltage is

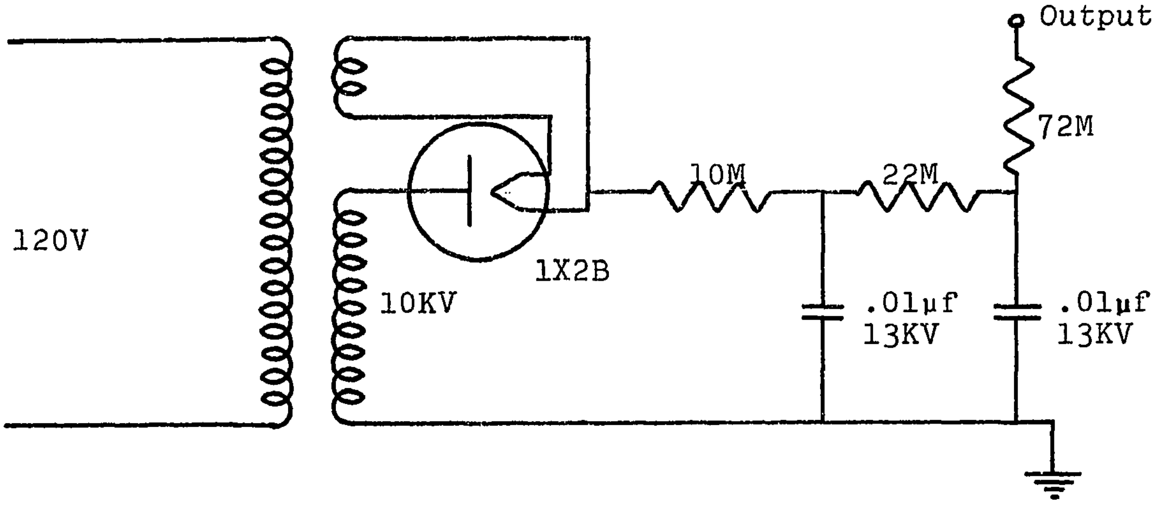

Figure 5-12. High voltage anode supply, 12KV, 50MA.

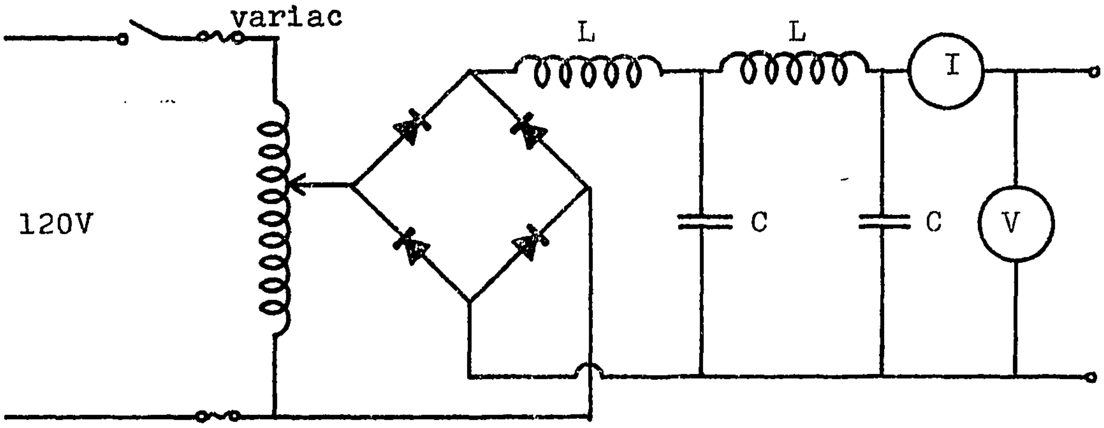

Figure 5-13. 75W Tungsten-Halogen lamp supply, low ripple, 0 to 30V, 6A.

produced and modulated at a low frequency by a rotating magnetic field. This circumvents the problem of D.C. drift which is characteristic of high resistance photoconductors. The electric field in the sample depends upon the illumination, is generally not uniform, and changes with photoexcitation. Hence, it is desirable to measure only the A.C. component produced by the alternating magnetic field. The high resistivity of the samples requires a low frequency modulation to prevent capacitive loading by the circuit.

The photoconductivity and Hall mobility apparatus is shown in Figure 5-14. The sample X, is attached on the end of a quartz light pipe inside a vacuum jacket (the crystal mounting assembly). The crystal mounting assembly is positioned in a dewar so that the crystal is in the field of the rotating permanent magnet M. Two light sources are directed onto the top of the light pipe by diagonal mirrors m, one for primary excitation and the other for secondary or quenching radiation. The crystal is connected by ohmic contacts and fine wires to vacuum tight coaxial fittings at the top of the sample assembly, Figure 5-16.

The electrical system is shown in block form in Figure 5-15. The battery control supplies a constant voltage across the two ends of the crystal. The Hall voltage, at the center contact, is monitored by the detection system. Due to high sample resistance, the Hall voltage signal must not be loaded by the circuit. An electrometer of $10^{14}\Omega$ input resistance is used as a unity gain impedance matching device, or voltage

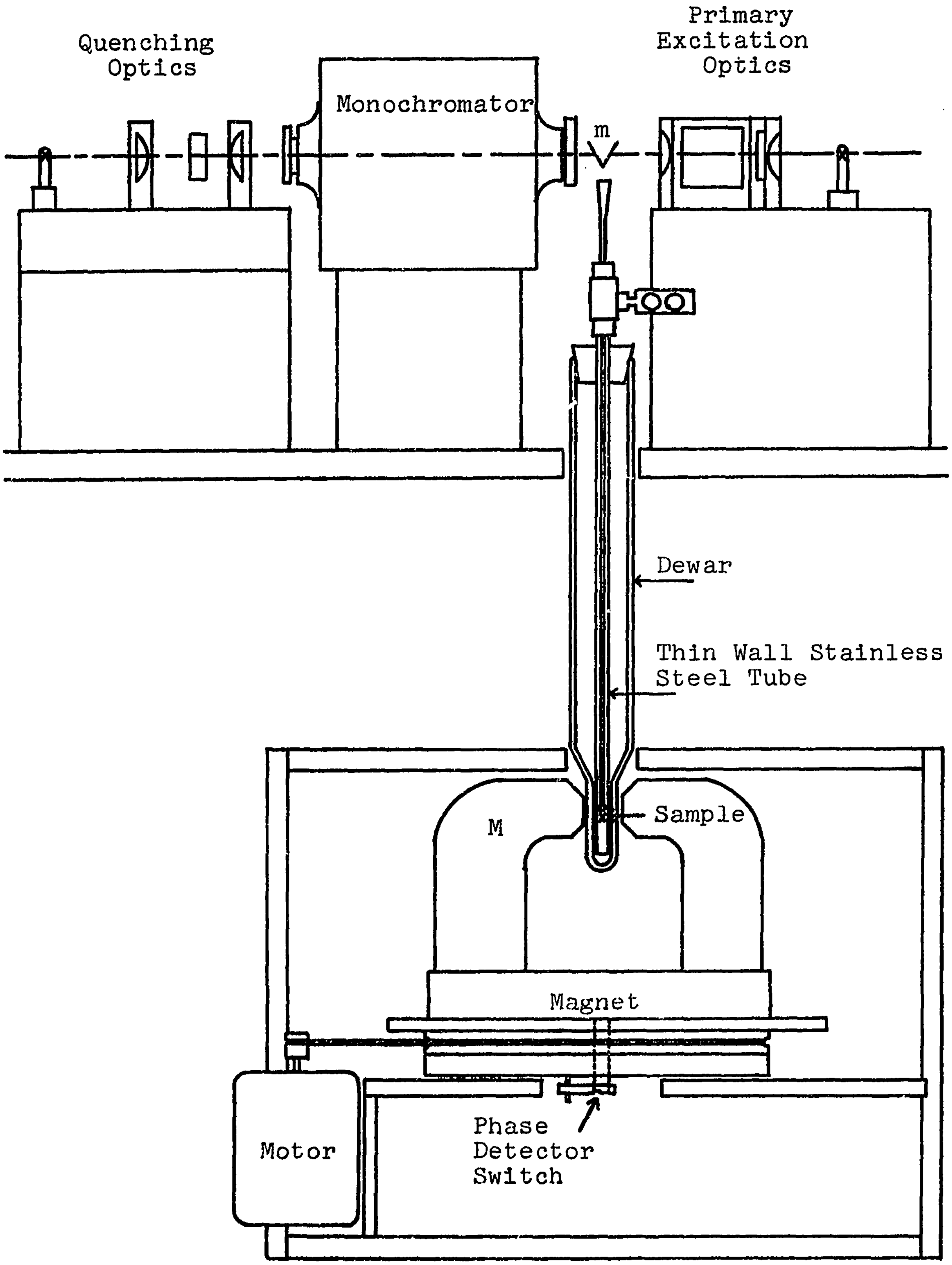

Figure 5-14. Sketch of the Hall mobility apparatus.

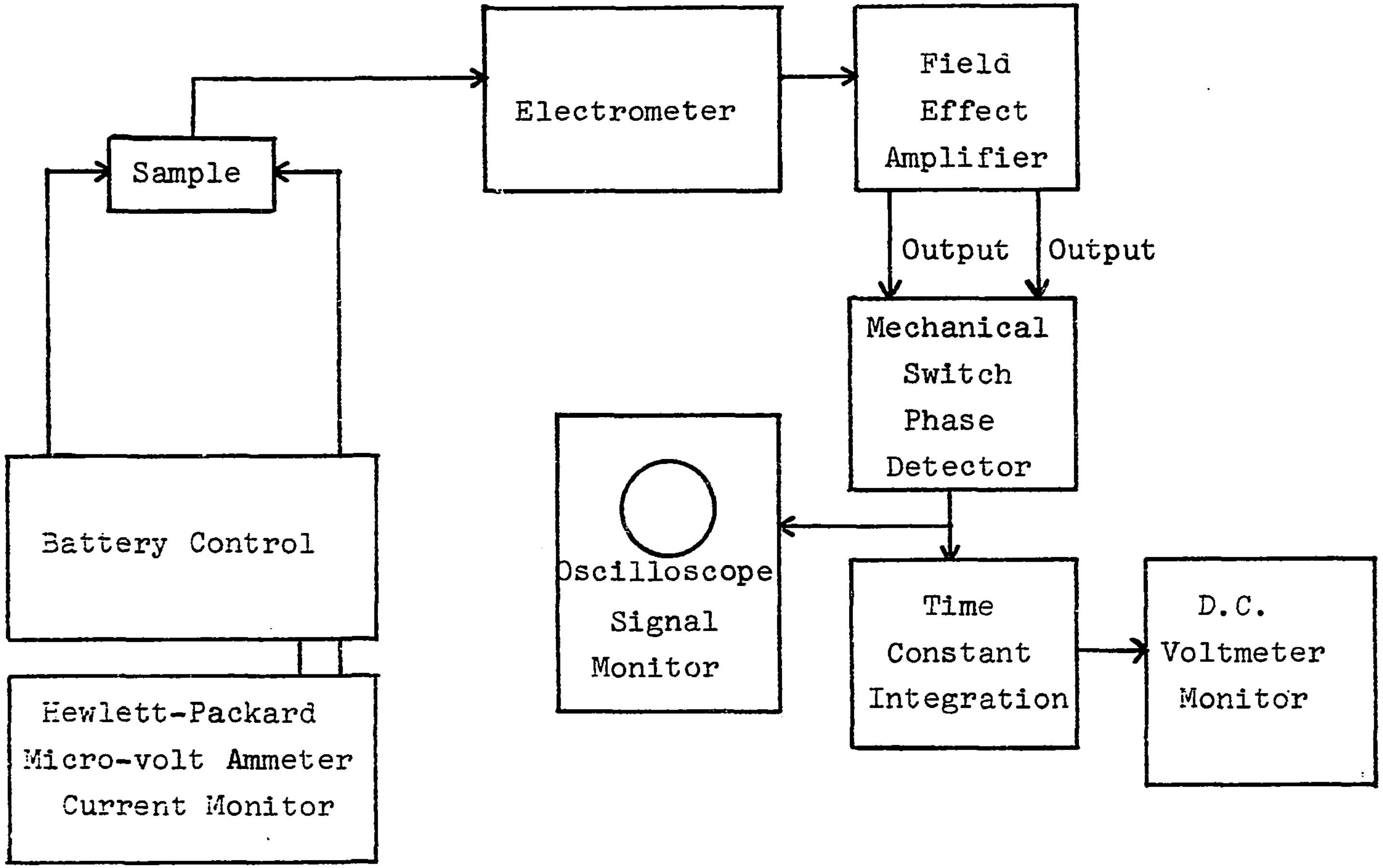

Figure 5-15. Block diagram of the Hall effect circuit.

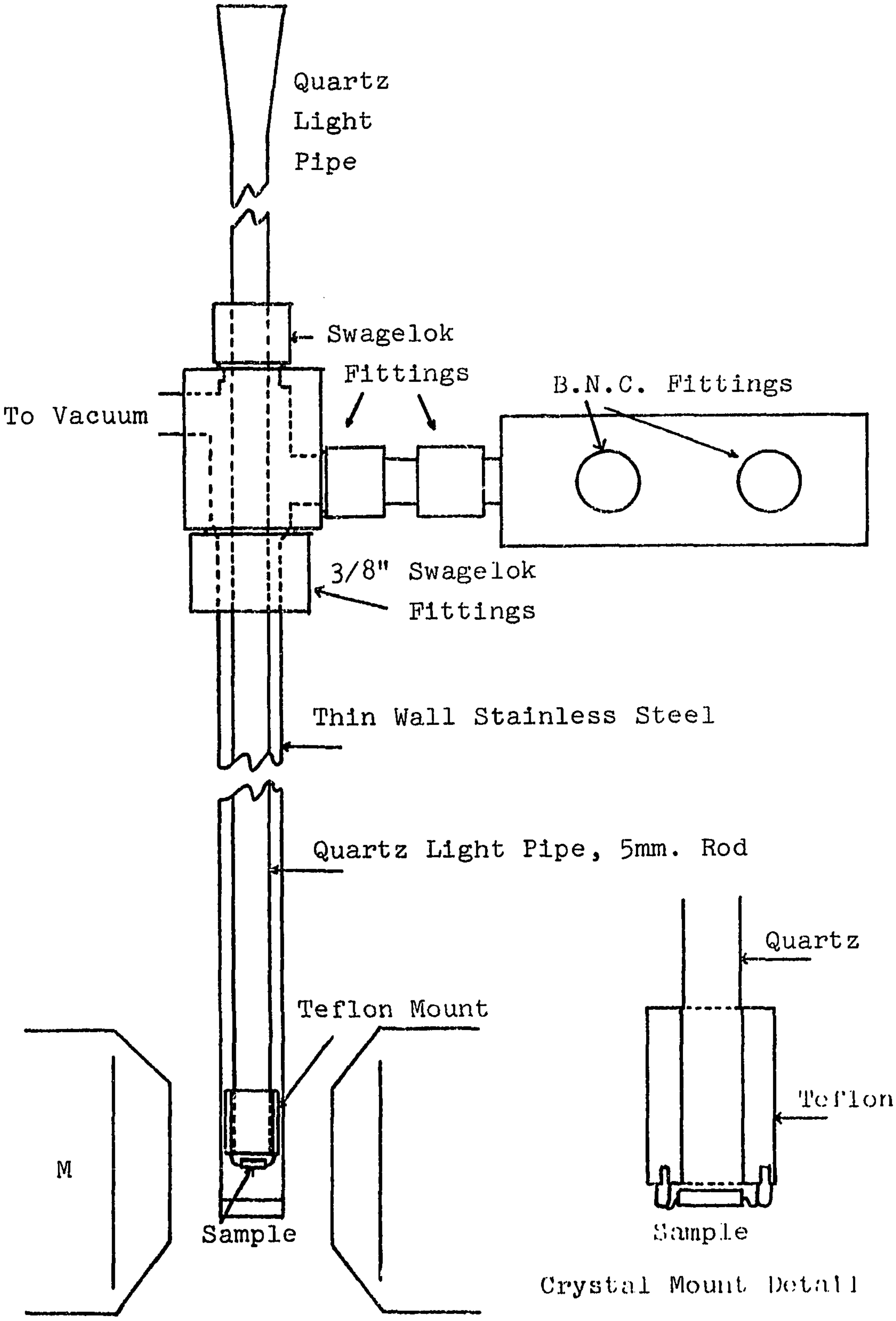

Crystal Mount Detail

Figure 5-16. The crystal mount assembly.

follower. It transforms the Hall voltage to a low impedance signal which is then fed to a low noise amplifier. The inverting and noninverting outputs of the amplifier are mechanically phase detected by a single pole double throw switch which is actuated by the rotating magnet. The rectified signal is integrated and monitored using a D.C. voltmeter. The phase detected signal is monitored on an oscilloscope. All connections are made with coaxial cable to prevent extraneous pickup, and all cases are connected to a common ground except the microvolt-ammeter I, which is not grounded.

The sample holder, Figure 5-16, is constructed of a brass body, commercial Swagelok* fittings, and a thin wall stainless steel tube. Parts are silver soldered together and the fittings are tightened by hand. The 0.005 inch thin wall stainless steel tube prevents excessive heat loss at low temperatures and provides good electrical shielding.

A quartz light pipe is used to transmit light from 0.3μ to 3.5μ. Pyrex is unsuitable for this application since it has higher attenuation in the near infrared. The crystal is mounted in contact with the light pipe, producing uniform illumination. The top of the rod is flared to 0.5 inch to accept the two light beams.

The three wires to the crystal are connected to pressure B.N.C. fittings so the holder can be evacuated and flushed with dry gas. Helium is used for low temperature measurements.

---

*Trademark of Crawford Fitting Co., Cleveland, Ohio.

The sample is mounted by its leads to the teflon insulator which fits snugly on the end of the light pipe as seen in the crystal mount detail, Figure 5-16.

The permanent magnet rotates at a constant speed on a ball bearing mount and is driven by an induction motor and rubber belt. The magnet rotates at about two cycles per second. It is mounted independently, not mechanically connected to the sample assembly, in order to isolate vibration. The phase detector switch is mounted below the magnet and is switched by a cam rotating with the magnet. The phase is adjusted by rotating the switch mounting wheel; and the switching symmetry is adjusted by a screw which moves the switch with respect to the rotating cam.

Two light sources are used consisting of a lamp, monochromator, and focusing lenses. The lamps used are 75 W tungsten-halogen quartz lamps as in the luminescence experiment. They are convenient due to their small size and low noise characteristics. Their high brightness is not as necessary for photoconductivity as it is for luminescence quenching. The optical block assemblies used are the same as for the luminescence equipment.

Since quenching light requirements are less for photoconductivity measurements, a grating monochromator is used; giving better resolution than the thin film dielectric filters. Four gratings were available allowing coverage from 0.3μ to 3μ. Broad band interference filters were used to isolate unwanted orders. A thin film filter is used to select primary excitation wavelength. For the intensity dependence study, a motor driven flag was used which slowly attenuated the incident light.

The battery control box applies voltage to the sample, Figure 5-17. Voltage is variable from zero to the full battery voltage of 90 V. The voltage to the sample can be reversed by the reversing switch, to check for ohmic contacts. The D.C. component of the voltage at the Hall terminal may be balanced by the balancing resistor. This allows one to monitor the D.C. Hall voltage if the noise level permits. In general, spurious low frequency signals prevent D.C. measurement, and the balance control is adjusted so that the ammeter is grounded to minimize 60 Hz pickup. The amplifier is capacitively coupled so the D. C. component of the applied voltage appearing at the Hall terminal is eliminated.

The micro-ammeter measures the crystal current, and is sufficient for measuring photoconductivity in sensitive samples. The electrometer used was a Keithley 610B, with input resistance of $10^{14}\Omega$ and a voltage scale of 100 V. It has a unity gain output of low impedance which serves as the input to the amplifier.

The amplifier is similar to the luminescence signal amplifier, except that it is untuned and a voltage divider input network gives gain ranges of 10, 30, 100, 300, and 1000. The output signal is phase-split and synchronously rectified. The rectified signal is integrated with a time constant of about 5 seconds.

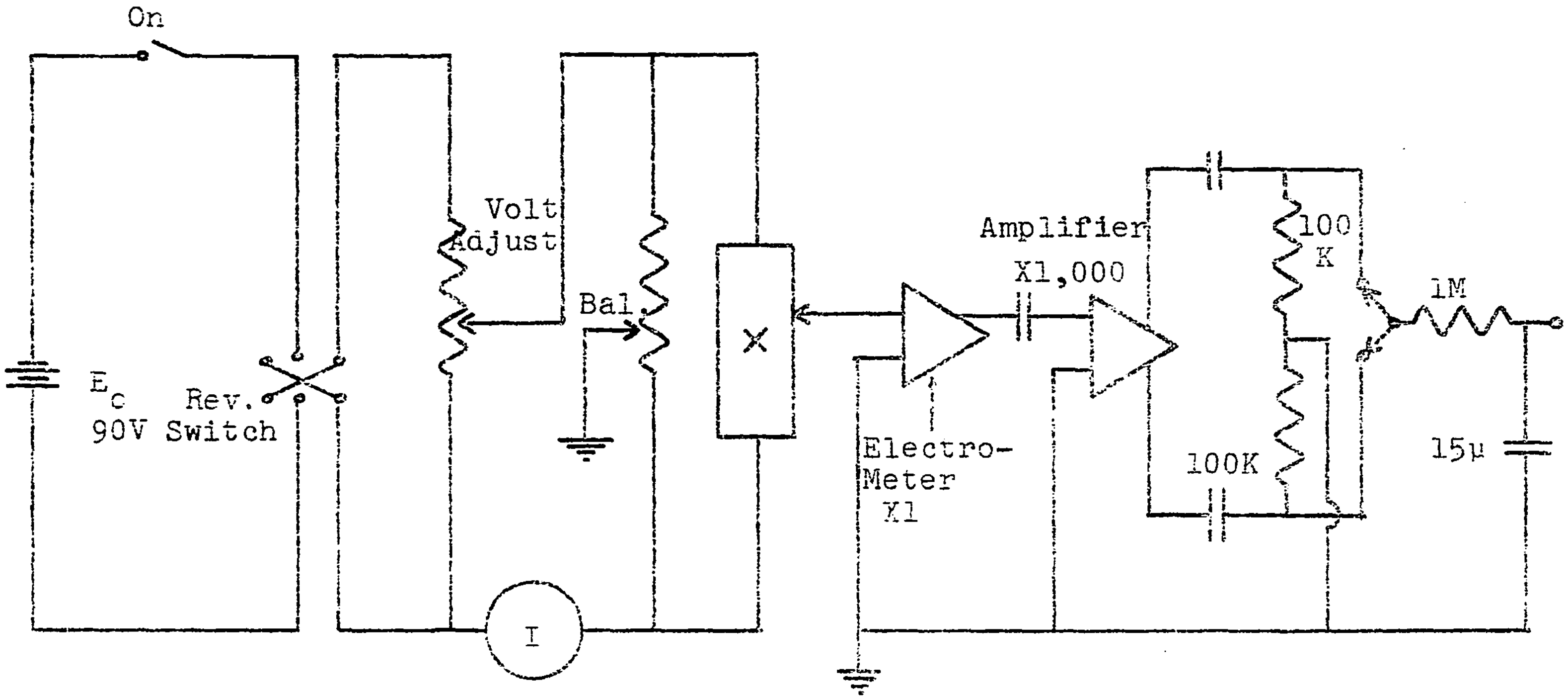

Figure 5-17. Electrical circuit of Hall mobility apparatus.

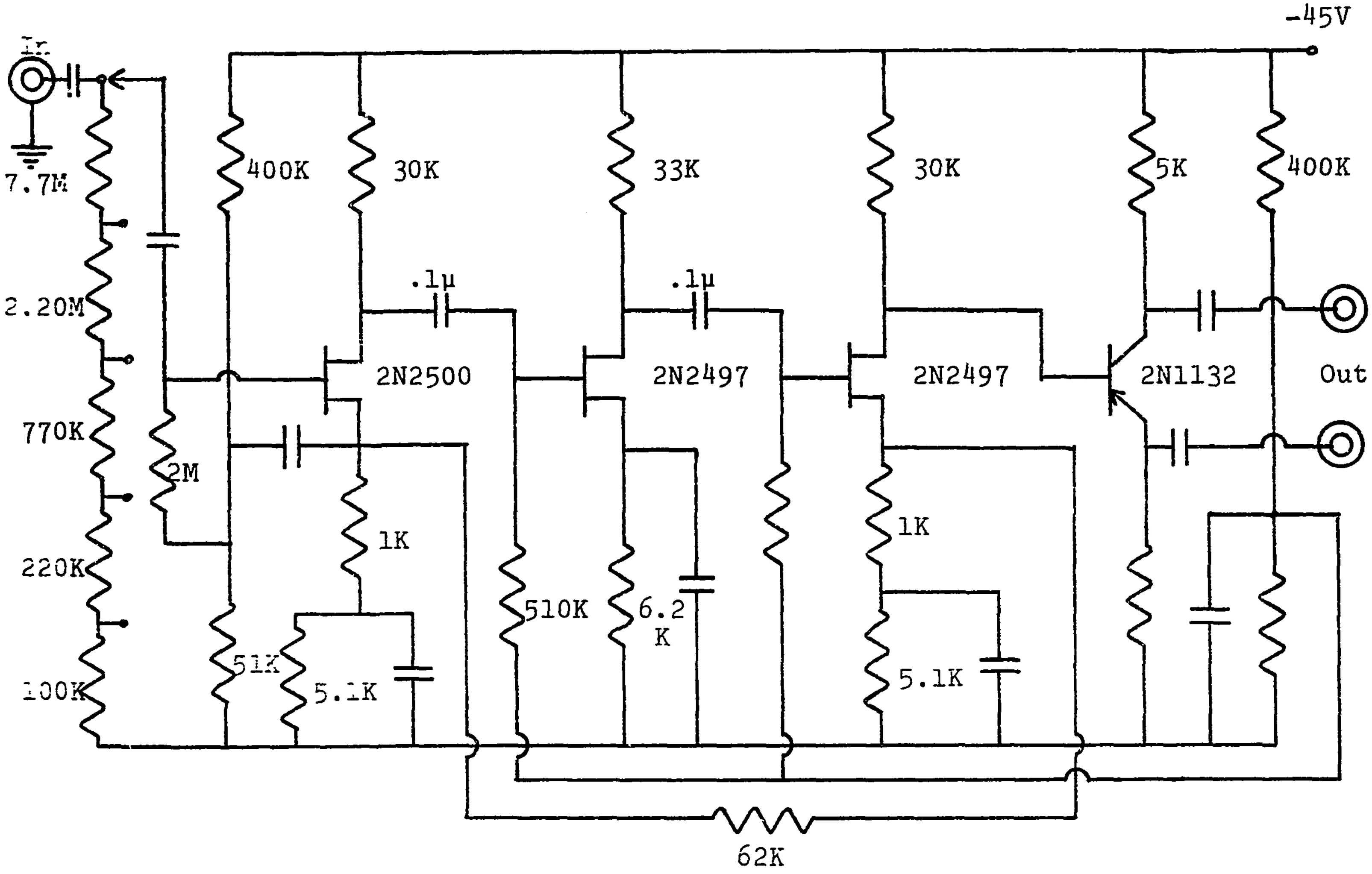

Figure 5-18. Field effect transistor amplifier.

Crystal preparation. Samples may be prepared for measurement by cutting or cleaving, or may be used as irregular shapes. Although irregular crystals are difficult to use, many of the samples were too small to cut or cleave and were used in their original shape. For most CdS crystals, samples were cut to a standard size of 1 x 1 x 5 mm, using a wire saw with abrasive slurry.

Prior to doping or attaching of contact, crystals must be cleaned. The general procedure is to clean in a solvent, such as trichlorethylene, followed by a light etch in hydrochloric acid and rinsing in distilled water. ZnS crystals must be etched in hot hydrochloric acid.

Several methods for contact preparation were examined; including silver paste, pressed indium, evaporated indium, and indium fired at high temperatures in hydrogen gas. The only satisfactory contacts for ZnS were made using melted indium baked at about 500°C in $H_2$ (40). These were fairly ohmic with low voltage drop at the contacts. For CdS, pressed or melted indium contacts were satisfactory. Small copper wires were soldered to the contacts during preparation and the crystals were mounted by the lead wires.

# CONCLUSIONS

The two crystal-field energy levels of the $(3d)^9$ state of $Cu^{++}$ in the ZnS crystal lattice relative to the valence band is shown in Figure 4-8. A new quenching band in the 2.3μ-2.5μ region has been observed for the green luminescence of ZnS:Cu:Cl. This may be ascribed to the transition of holes from the lower crystal-field level of $Cu^{++}$ to the valence band. All three quenching bands of the green luminescence (0.8μ, 1.3μ, 2.4μ) are accompanied by an initial stimulation. It is suggested that the stimulation effect may be explained as the results of transfer of holes from the slow to the fast luminescence centers using the unassociated pair model.

Three quenching bands at 0.8μ, 1.4μ, and 2.4μ have been observed for the 1.0μ luminescence of CdS:Cu:Cl. These can be explained in terms of the crystal-field energy levels of $Cu^{++}$ in CdS lattice similar to the case of ZnS.

Quenching of photo-Hall effect by 0.8μ and 1.3μ-1.4μ radiation has been observed for both ZnS:Cu:Cl and CdS:Cu:Cl. The reduction of the Hall mobility may be interpreted as the introduction of hole conduction produced by the infrared radiation.

## REFERENCES

1. Curie, D., *Luminescence in Crystals*. John Wiley & Sons Inc., New York (1963).
2. Kang, C.S., Phipps, P.B.P., and Bube, R.H., Phys. Rev. **156**, 998 (1967).
3. Shionoya, S., Era, K., and Washizawa, Y., J. Phys. Soc. Japan **21**, 1624 (1966).
4. Era, K., Shionoya, S., and Washizawa, Y., J. Phys. Chem. Solids **29**, 1827 (1968).
5. Era, K., Shionoya, S., Washizawa, Y., and Ohmatsu, H., J. Phys Chem. Solids **29**, 1843 (1968).
6. Weakliem, H.A., J. Chem. Phys. **36**, 2117 (1962).
7. Broser, I., Maier, H., and Schulz, H.J., Phys. Rev. **140** A2135 (1965).
8. Browne, P.F., J. Electron. **2**, 1 (1956).
9. Meijer, G., J. Phys. Chem. Solids **7**, 153 (1958).
10. Aven, M. and Prener, J.S., *Physics and Chemistry of II-VI Compounds*, John Wiley & Sons Inc., New York, 1967, Chapter 3, p. 138.
11. Ref. 10, Chapter 13, p. 660.
12. Balkanski, M., Gans, F., *Luminescence of Organic and Inorganic Materials*. International Conference, New York University, Washington Square, Edited by H.P. Kallmann and G.M. Spruch, John Wiley & Sons Inc., New York, (1962).
13. Van Gool, W., Thesis, Univ. of Amsterdam, Jan. 1961,

Phillips Research Reports, Suppl. 1961, No.3, Phillips Research Laboratories, p. 3.

14. Ref. 1, p. 114.
15. Ref. 1, p. 119; W. Van Gool, Phil. Res. Rep. 13 157.
16. Garlick, G.F., and Dumbleton, M.J., Proc. Phys. Soc. London B67 442 (1954).
17. Apple, E.F., and Prener, J.S., J. Phys. Chem. Solids 13 81 (1960).
18. Weakliem, H.A. and McClure, D.S., J. Appl. Phys., Suppl. 33 347 (1962); Weakliem, H.A., J. Chem. Phys. 36 2117 (1962).
19. Shionoya, S., Internatl. Luminescence Conf. Budapest, Aug. 1966; Shigeo Shionoya, in *Luminescence of Inorganic Solids* (edited by P. Goldberg), Chapter 4, p. 206, Academic Press, New york (1966).
20. Schon, M., Z. Physik 119 463 (1942); Klasens, H.A., Nature 158 306 (1946).
21. Lambe, J. and Klick, C., Phys. Rev. 98 909 (1955).
22. Prener, J.S., Weil, D.S., J. Electrochem. Soc. 106 409 (1959).
23. Hopfield, J.J., Thomas, D.G., and Gershenzon, M., Phys. Rev. Lett. 10 162 (1963); Thomas, D.G. Gershenzon, M., and Trumbore, F.A., Phys. Rev. 133 A269 (1964).
24. Bube, R.H., Phys. Rev. 80 655 (1950). Leverenz, H.W. *Luminescence of Solids* (Dover Publications Inc., New York, 1968).

25. Kang, Chang S., Phipps, Beverly P., and Bube, R.H., Phys. Rev. 156 998 (1967); Ref. 3, p. 213; Broser, I. and Broser-Warminsky, R., J. Phys. Rad. 17 791 (1956); Bube, R.H., Phys. Rev. 99 1105 (1955).

26. Ref. 1, p. 161.

27. Frerichs, R., Naturwissenschaften 33 281 (1946).

28. Rose, A., Phys. Rev. 97 322 (1955).

29. Putley, E.H., The Hall Effect and Related Phenomena, Butterworth and Co., Ltd., London, 1960.

30. Samelson, H., J. Appl. Phys., 33 1779 (1962).

31. Yarger, C.R., private communication.

32. Morehead, F.F., J. Ph. Chem. Sol. 24 37 (1962); Ullman, F.G. and Dropkin, J.J., J. Electrochem. Soc. 108 154 (1961); Koda, T. and Shionoya, S., Phys. Rev. 136 A541 (1964).

33. Meijer, G., J. Phys. Chem. Sol. 7 153 (1958).

34. Kang, C.S., Ph.D. thesis, Stanford Univ. Dept. of Materials Sci., 1965.

35. Bryant, F.J. and Cox, A.F.J., Proc. Phys. Soc. (London) 87 551 (1966); Browne, P.F., J. Electron. 2 1 (1956).

36. Garlick, G.F.J., and Mason, D.F., J. Electrochem. Soc. 96 90 (1949); Era, K., Shionoya, S., Washizawa, Y., J. Phys. Chem. Sol. 29 1827 (1968): Era, K., Shionoya, S., Washizawa, Y., and Ohmatsu, H., J. P. C. S. 29 1843 (1968).

37. Bube, R.H., Macdonald, H.E., and Blanc, J., J. Phys. Chem. Sol. 22 173 (1961).

38. Infrared Detector Catalogue, Texas Instruments, Dallas, Texas.

39. Johnson, D.R., Ph.D. thesis, Univ. of Okla. 1967.

40. Blount, G.H., Fisher, M.W., Morrison, R.G., and Bube, R.H., J. Electrochem. Soc. 113 690 (1966).